

X-ray diffraction at the Z Facility and path to time-resolution



Tommy Ao

Marius Schollmeier

Sandia National Laboratories, Albuquerque, NM



*Exceptional
service
in the
national
interest*

National Diagnostics Working Group Meeting
November 29-30, 2016



Sandia National Laboratories is a multi-program laboratory managed and operated by Sandia Corporation, a wholly owned subsidiary of Lockheed Martin Corporation, for the U.S. Department of Energy's National Nuclear Security Administration under contract DE-AC04-94AL85000.

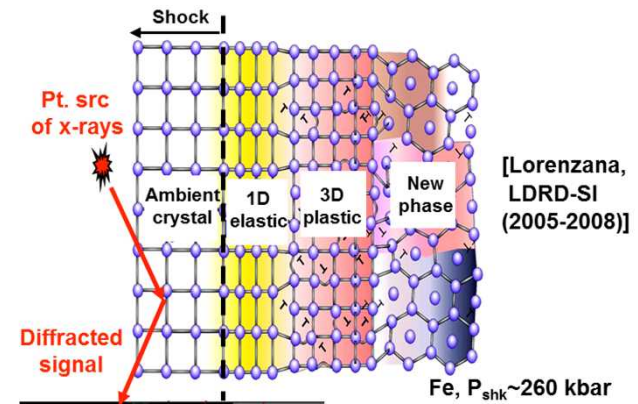
Outline

- Scientific Needs and Challenges
- Conceptual Design and Implementation of Z-XRD
- Ongoing Work and Developments

Scientific Needs and Challenges

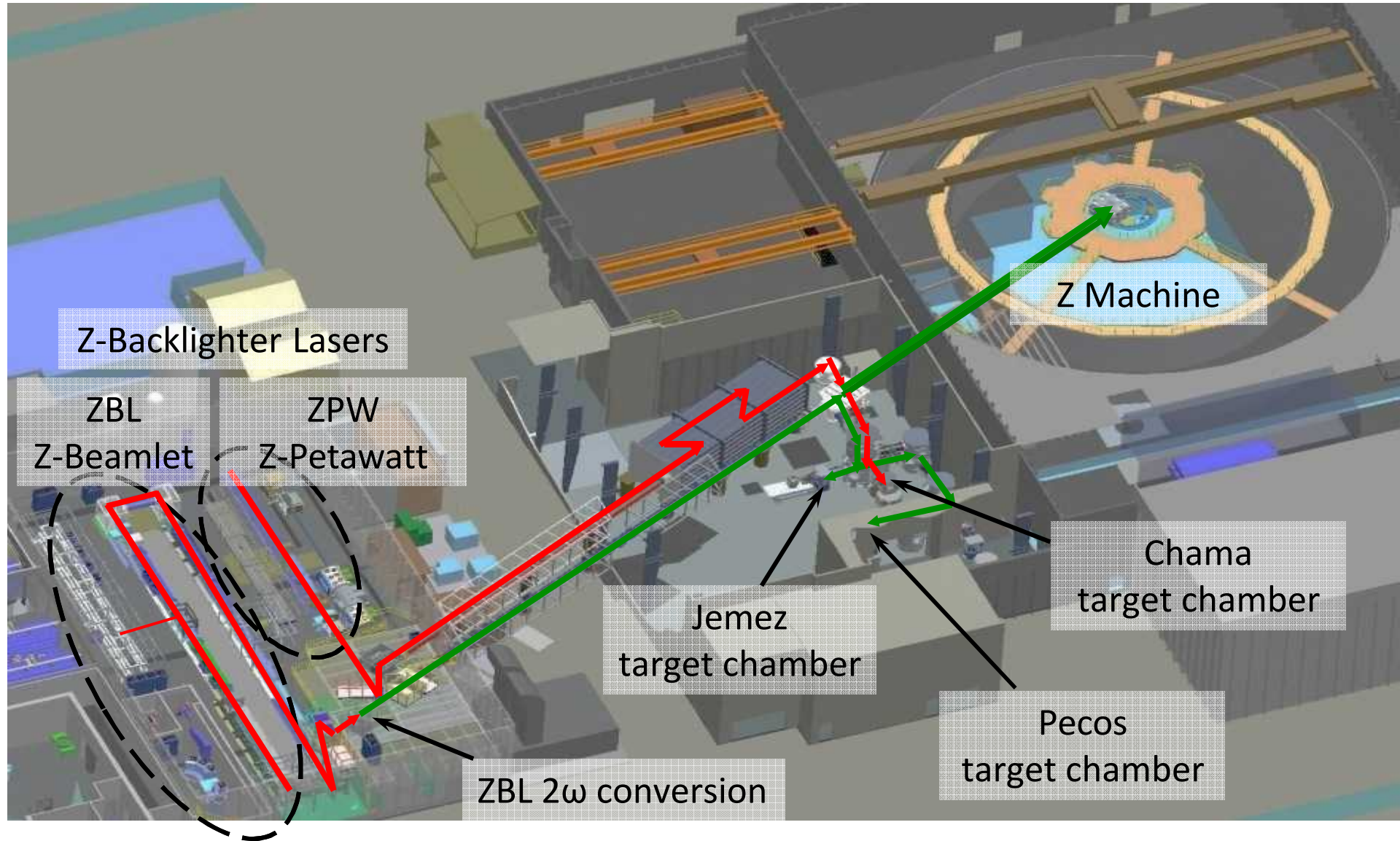
Purpose: diagnose material lattice dynamics during dynamic compression

- What?
 - Characterize phase transformations that occur in dynamically compressed condensed matter on **ns** time scales and **nm** spatial scales
- Why?
 - Such information enables to determinate how material behaves under extreme conditions
 - For most materials, there are very few constraints on existing models for phase transitions under dynamic loading
- How?
 - Perform time-resolved, x-ray diffraction measurements on dynamically compressed, polycrystalline matter



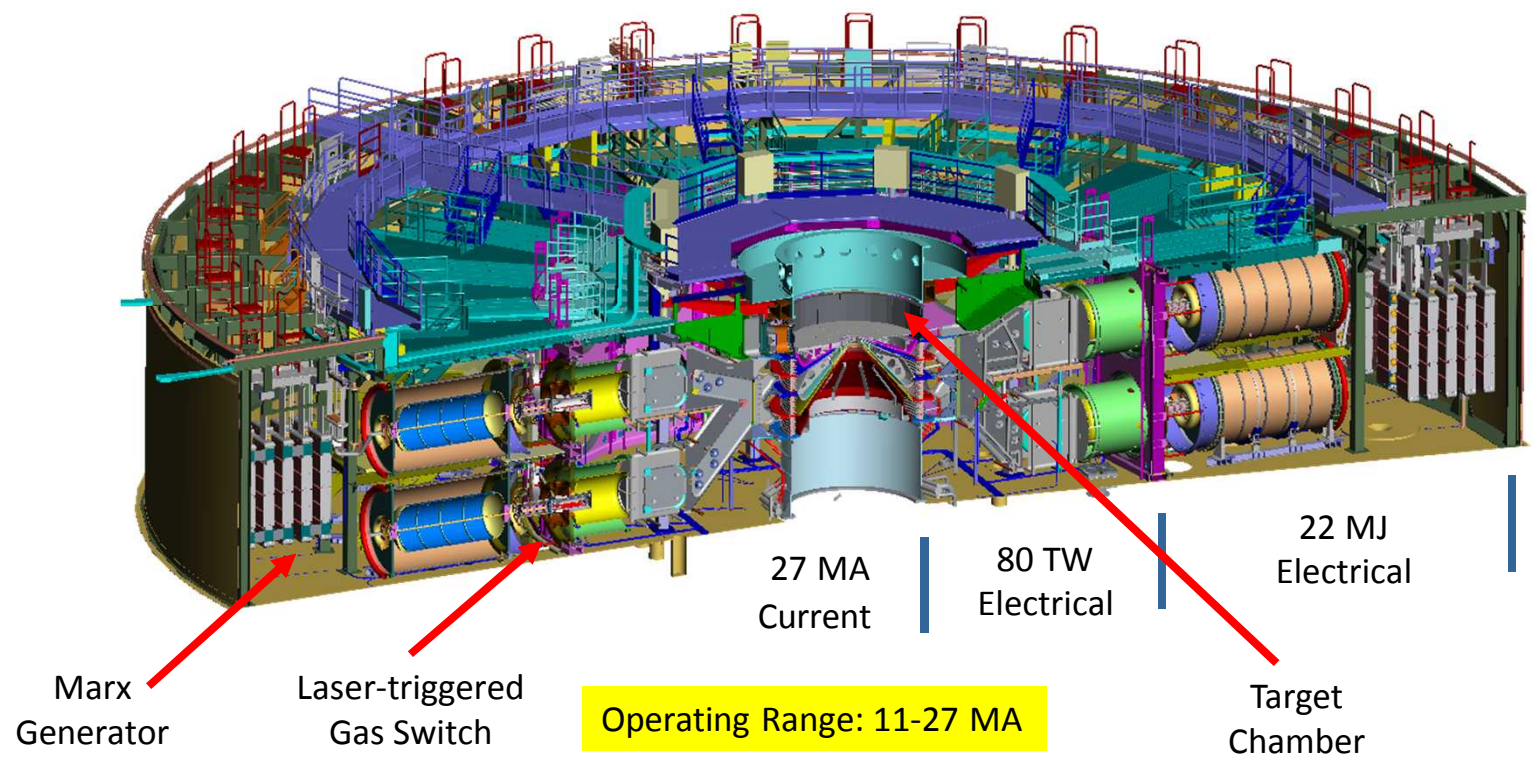
DXRD: Dynamic X-Ray Diffraction

Overview of Z Facility



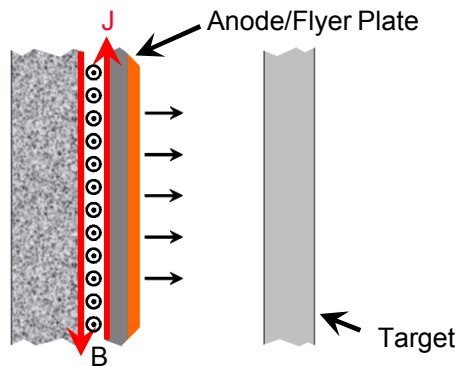
Combining x-ray diffraction with Z's unique HED samples will provide benchmark quality data

- Z's high energy density matter samples are large, uniform, long-lived and precisely characterized
- X-ray diffraction will expand diagnostic capabilities on Z beyond pressure and density measurements



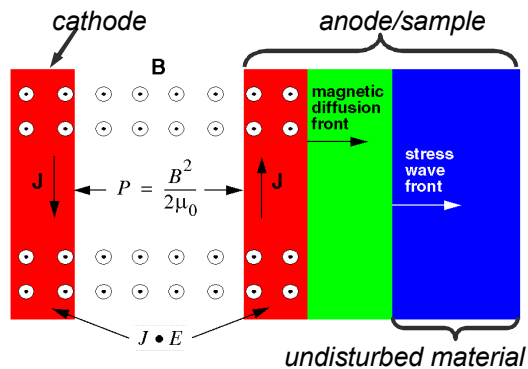
Z is a unique platform for EOS studies

- Dynamic material properties (DMP) experiments



- Magnetically launched flyer plates for shock compression¹

- Flyer impact velocities to ~ 40 km/s
 - Hugoniot states to ~ 10 Mbar; 10,000 – 50,000 K
 - Pressure and density characterized ~ 1-2 %



- Ramp (shockless) compression²

- Continuous quasi-isentropic compression to ~ 5 Mbar
 - Strain rates ~ 10⁶-10⁷ /s
 - Lower temperature states ~ 1000 – 3000 K

- Shock-ramp compression³

- Initial flyer impact followed ramp loading
 - Complex loading path access off-Hugoniot states
 - Shock melt and ramp refreeze

¹R.W. Lemke *et al.*, J. Appl. Phys. **98**, 073530 (2005)

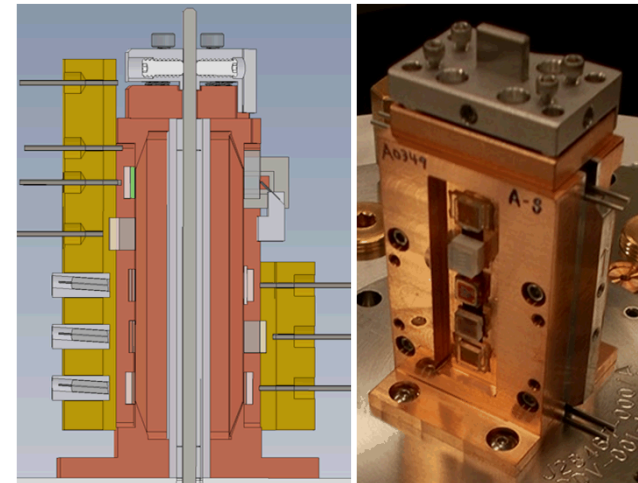
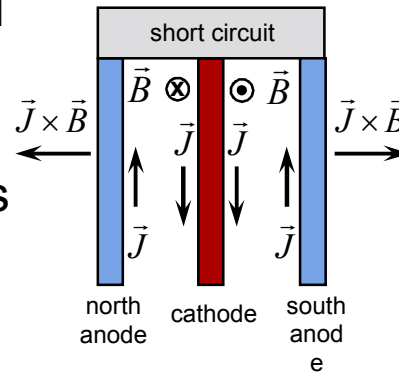
²J.-P. Davis *et al.*, Phys. Plasmas **12**, 056310 (2005)

³C. T. Seagle *et al.*, Appl. Phys. Lett. **102**, 244104 (2013)

Z-DMP planar experiments

■ Coaxial load

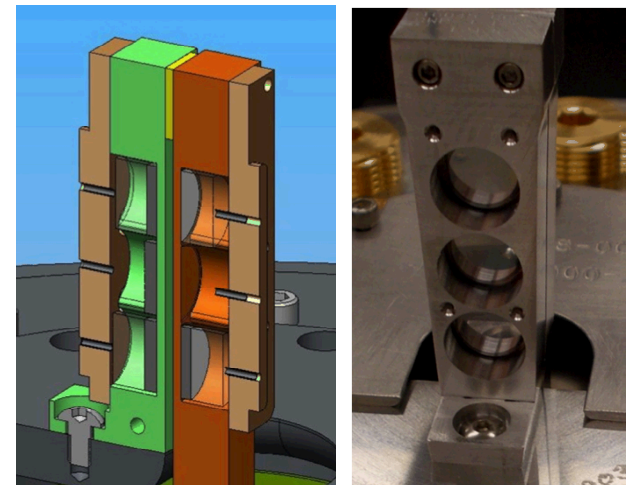
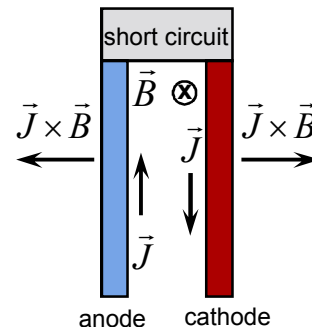
- Cathode stalk surrounded by anode panels
- Dual pressures possible on north and south panels
- More sample locations
- Enclosed magnetic fields, current and plasma flow



$$P = \frac{B^2}{2\mu_0}$$

■ Stripline load

- Identical pressure on both cathode and anode panels
- Higher current density and pressure
- Open magnetic fields, current and plasma flow



Challenges of XRD on Z-DMP experiments

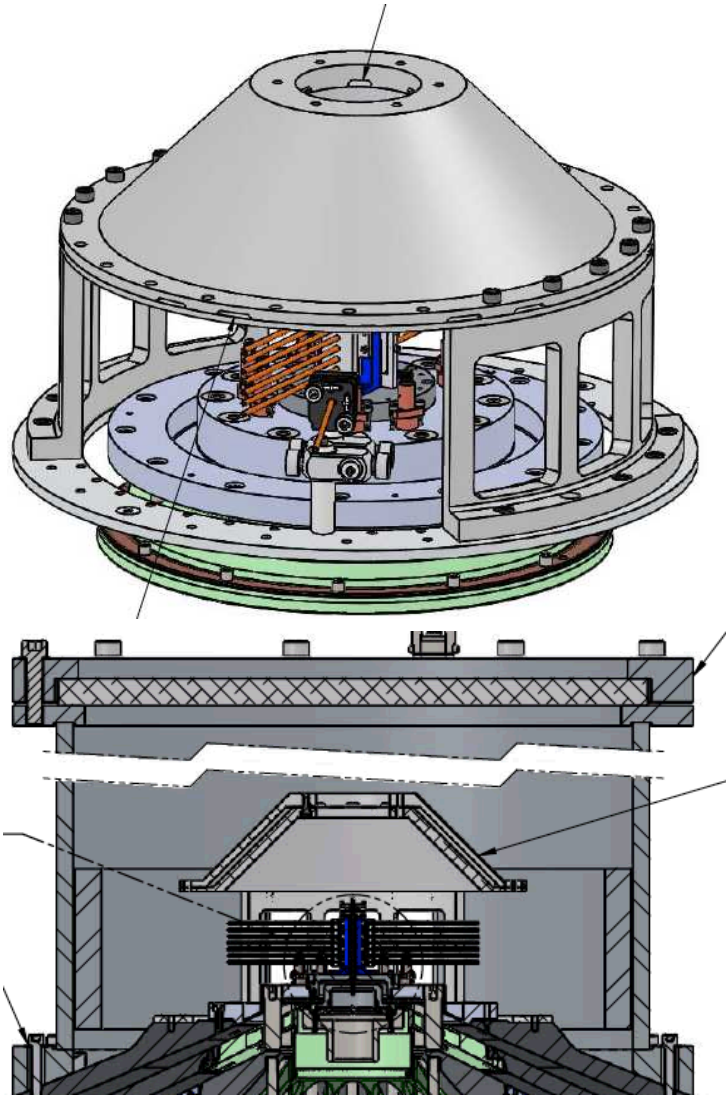
- Target parameters
 - Large and thick samples
 - High Z samples
 - Reflection geometry
 - Containment targets: inserting x-rays & extracting diffracted x-rays
- Destructive environment of Z-DMP load
 - Prevent catastrophic vacuum breach
 - Protect Z-Backlighter Laser
 - Retrieve data
- X-ray background
 - High energy photons (up to 10 MeV) produced
 - Sufficient signal-to-noise
- Electromagnetic pulse (EMP)
 - Fry electronics

Addressing challenges of Z-XRD

- High photon energy (>6 keV), short duration (~ 1 ns) multi-pulse x-ray sources (ZBL and/or ZPW)
 - Penetrate into thick and high Z targets
 - Temporally resolve phase transformations
- Placing image plate, x-ray CCD, or x-ray streak camera near load
 - Advanced debris mitigation
 - Robust x-ray and EMP shielding
- Convert diffracted x-rays into visible photons
 - X-ray phosphor/scintillator near load
 - Transport optical light out of load region (open optics)
 - Record light on optical CCD away from debris, x-ray background and EMP field

Z-DMP ridealong tests on Z2959

- Debris Witness Assembly



Z2959: Debris witness assembly post-shot

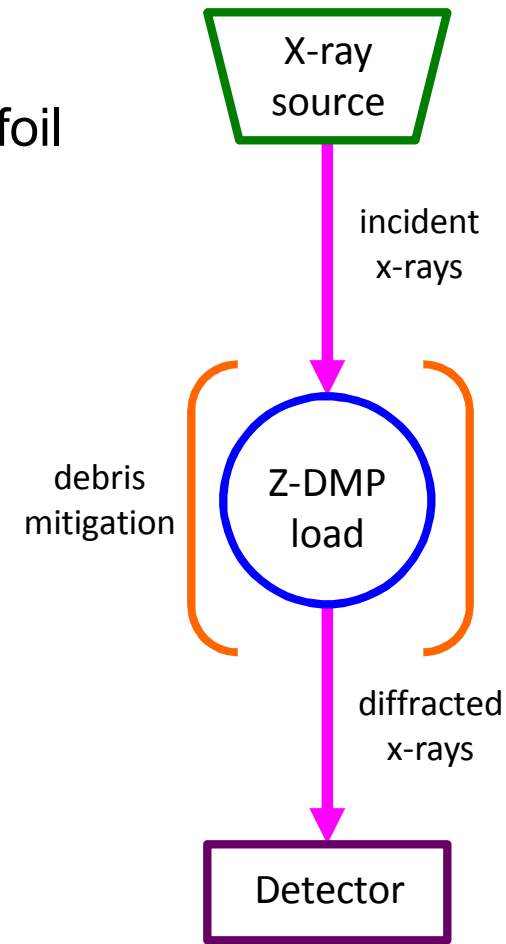
- Protection and recovery of any XRD detector near Z-DMP load highly unfeasible
 - e.g. image plate, x-ray CCD, x-ray streak camera



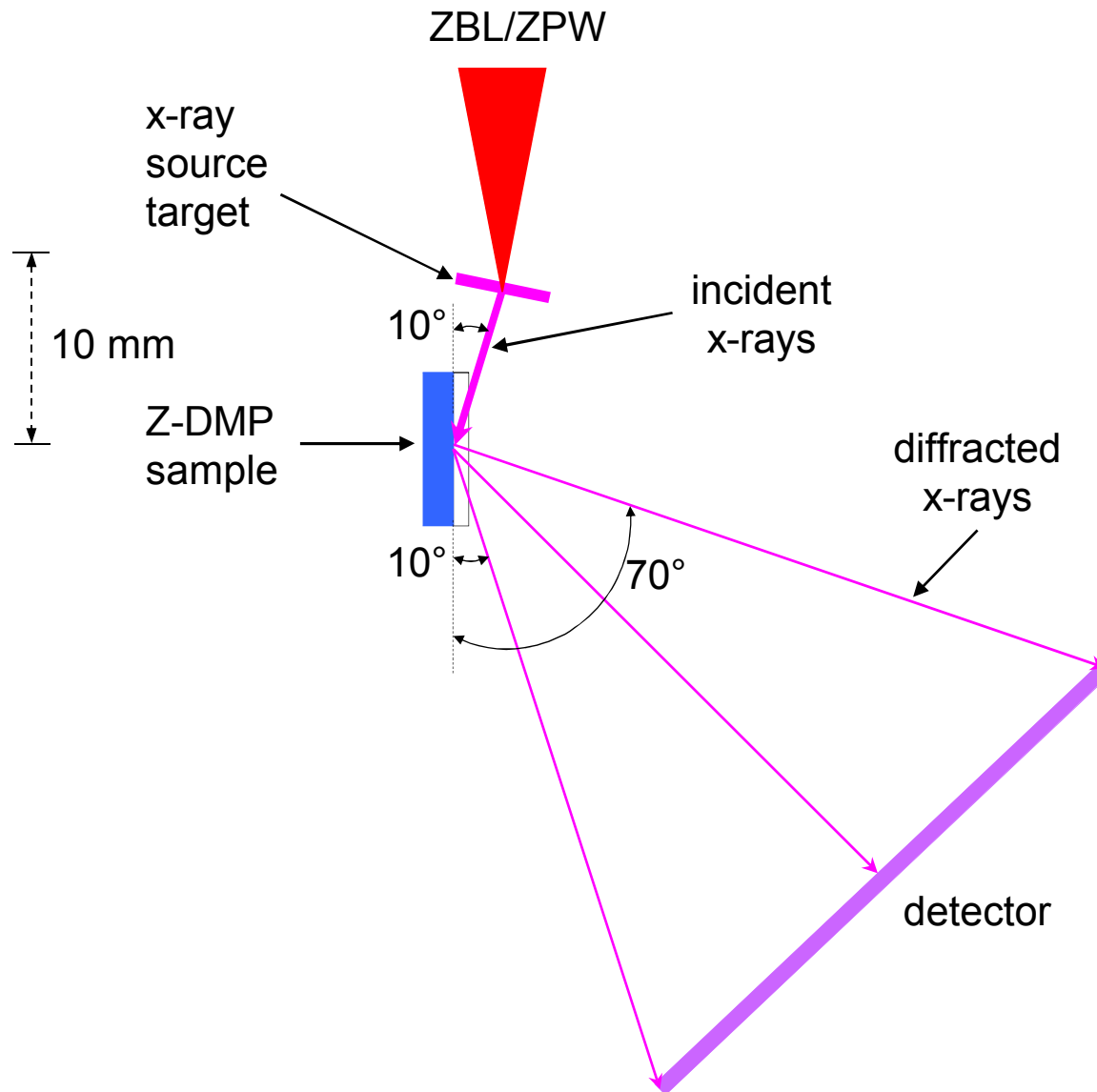
Conceptual Design and Implementation of Z-XRD

Three key components of XRD on Z-DMP experiments

- Produce source x-rays
 - Laser (ZBL/ZPW) irradiated metal foil
- Generate high-pressure state
 - Z-DMP load
 - Debris mitigation
 - X-ray background
- Detect diffracted x-rays
 - Scintillator/phosphor
 - CCD camera



General experimental design of Z-XRD

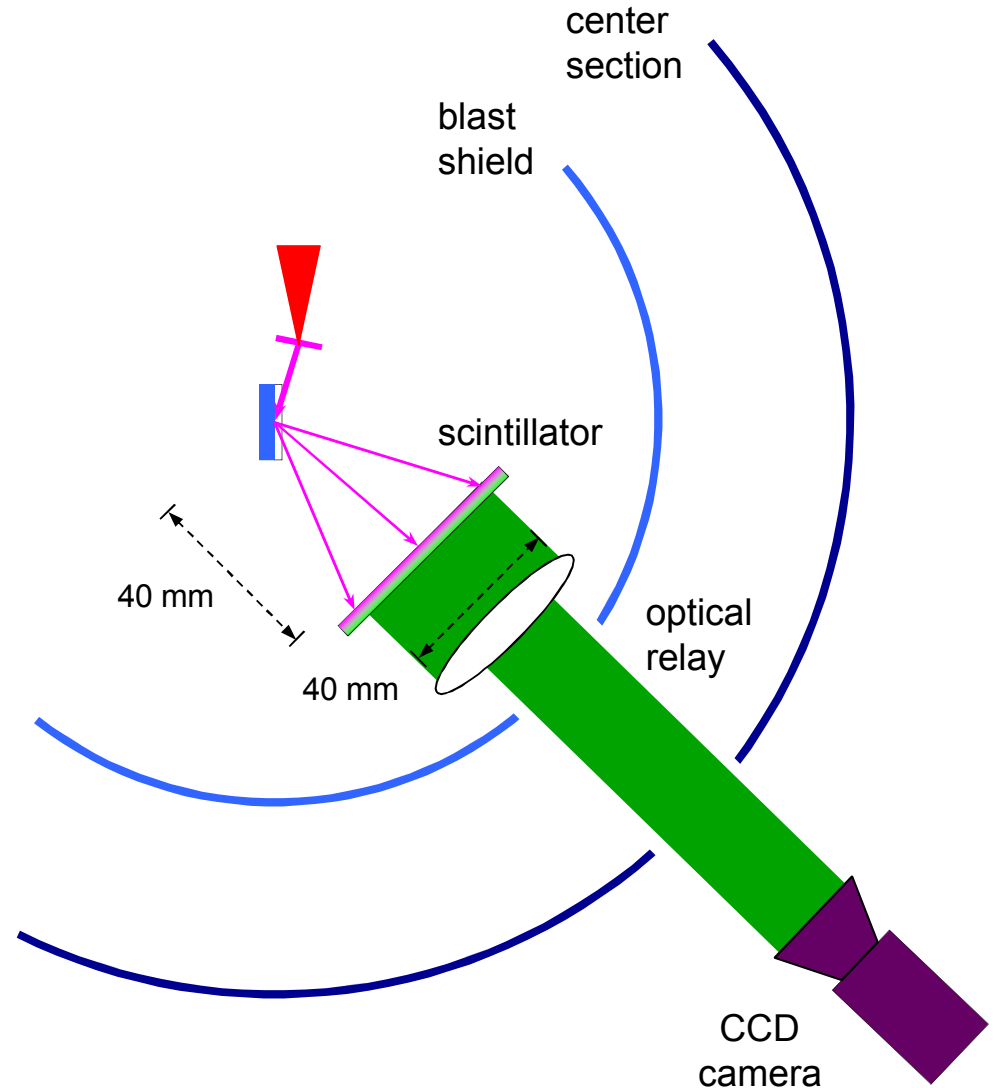


Z-XRD using scintillator/optical relay/CCD camera

- Operation
 - Scintillator located close to sample inside blast shield
 - X-ray conversion to optical light
 - Optical relay to outside blast shield and center section onto CCD camera

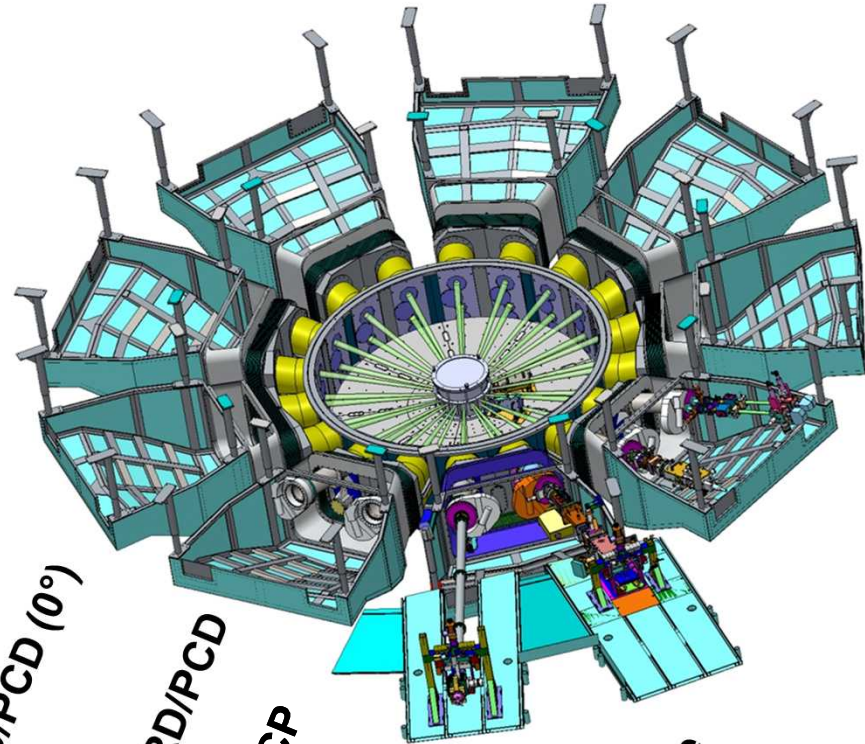
- Advantages
 - Time gating, possible multiple events

- Disadvantages
 - Optical background mitigation
 - Scintillator and optics destroyed
 - Alignment considerations

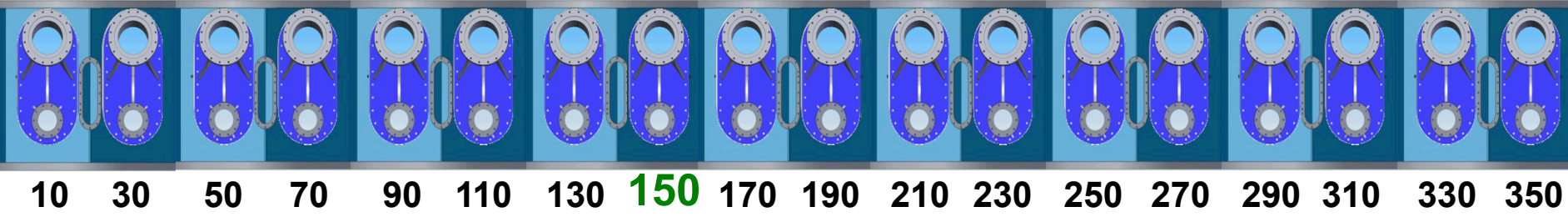


Radial LOS overview of the Z facility

- In-chamber diagnostics:
 - CRITR, TiGHER, SVS, DAHX
 - Neutron Activation (In and Cu)
 - VISAR, PSBO
 - Monochromatic Backlighter
 - TIPC
- 18 line-of-sight access ports at $\sim 12^\circ$
- 18 line-of-sight access ports at $\sim 0^\circ$

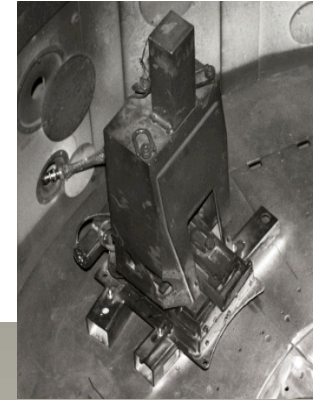
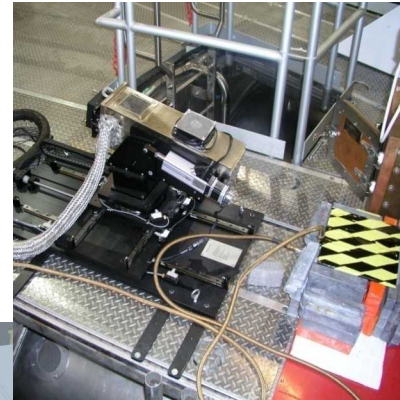
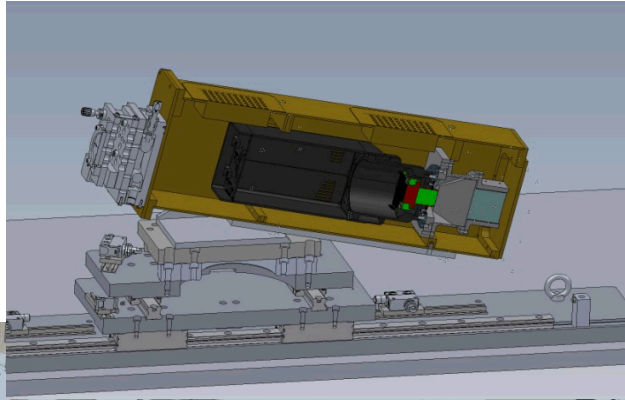
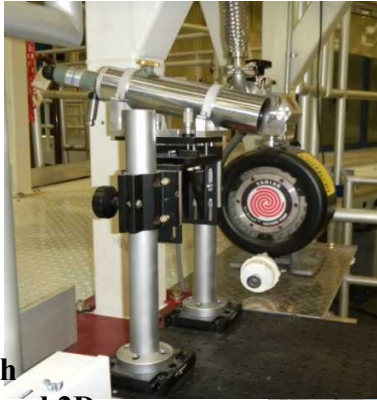


Cryo and Gas Puff
 Future
 Open Beam VISAR
 BOLO/XRD/PCD/TEP,
 nTOF
 VISAR
 Electrical Feedthrough
 SVS
 TIXTL
Neutron Imager
 MLM
 Bolo/XRD/PCD (0°)
 Open
 BOLO/XRD/PCD
 Gated MCP
 Open
 NTOF
 GMPC
 Be-Probe
 TREX



10 30 50 70 90 110 130 150 170 190 210 230 250 270 290 310 330 350

Neutron Imager at LOS150

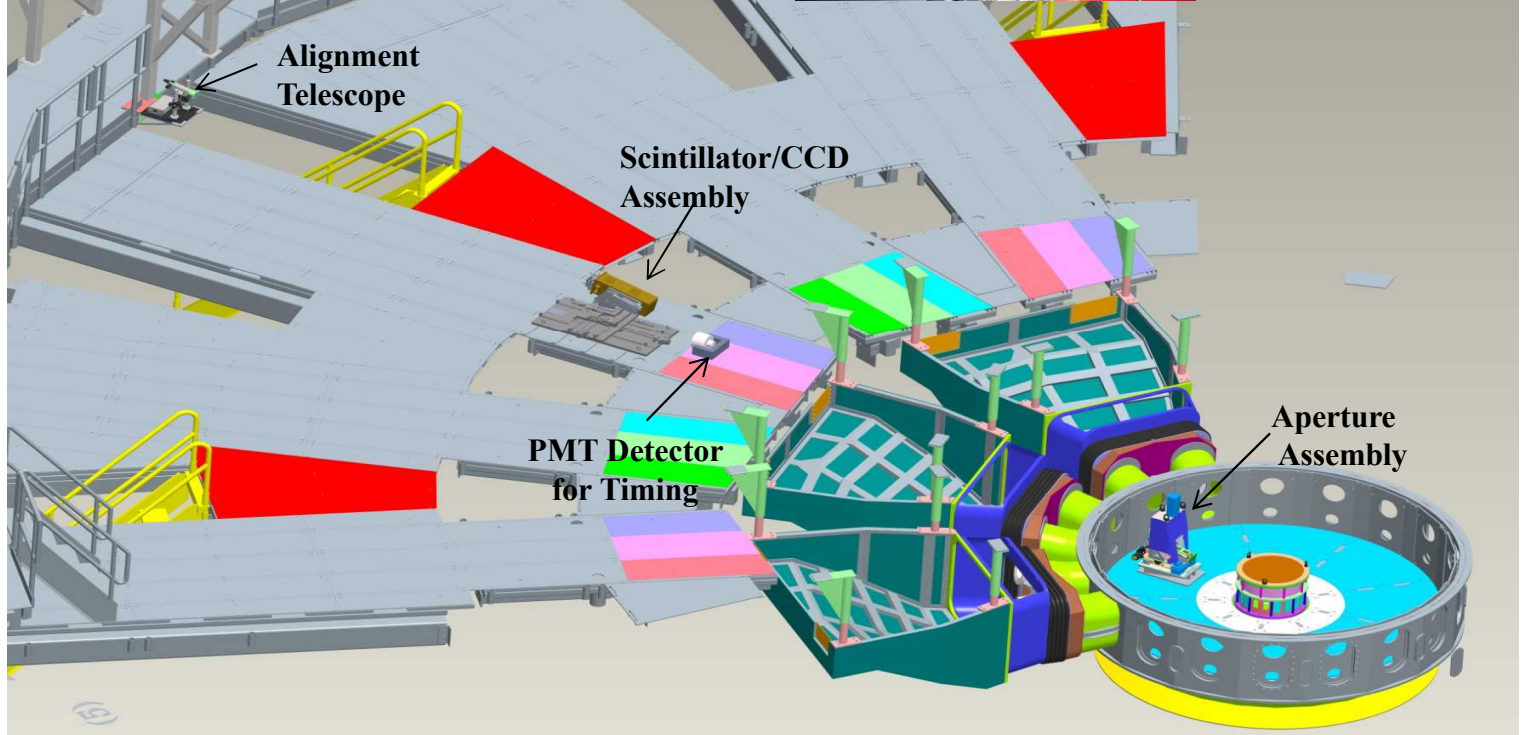


Both
1D and 2D
Apertures
Are Available

1D Aperture Is 204
Microns By 1 cm.
2D Aperture Is 152
Micron.
Overall Length Of
Aperture Is 15 Inches.
Aperture Straight
Section Is 1.8 cm.
Material Is
Tungsten.

Resolution For Either
Is Slightly Less Than
300 Microns.

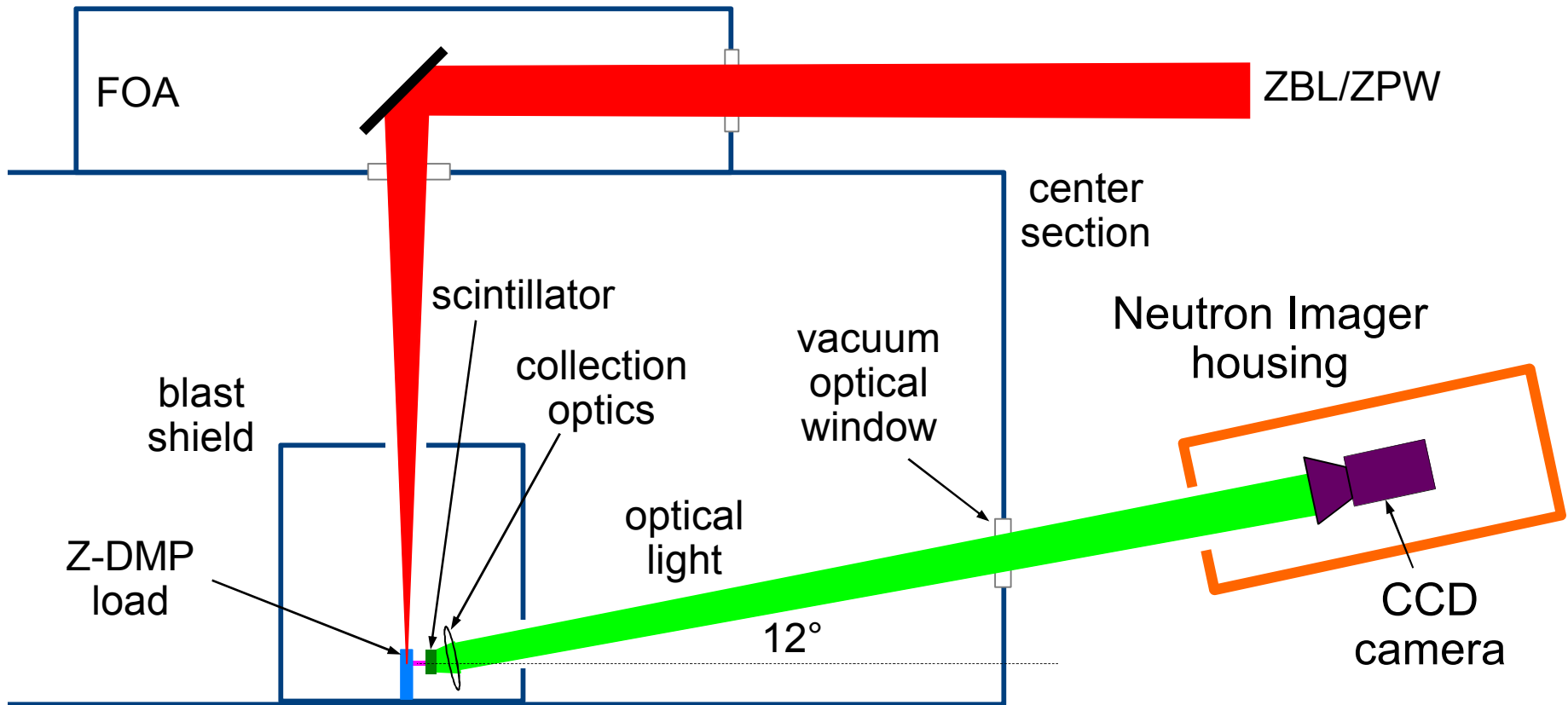
Imaging Scintillator
Is 2 Inch Cube That
Has 250 Micron Pixels.



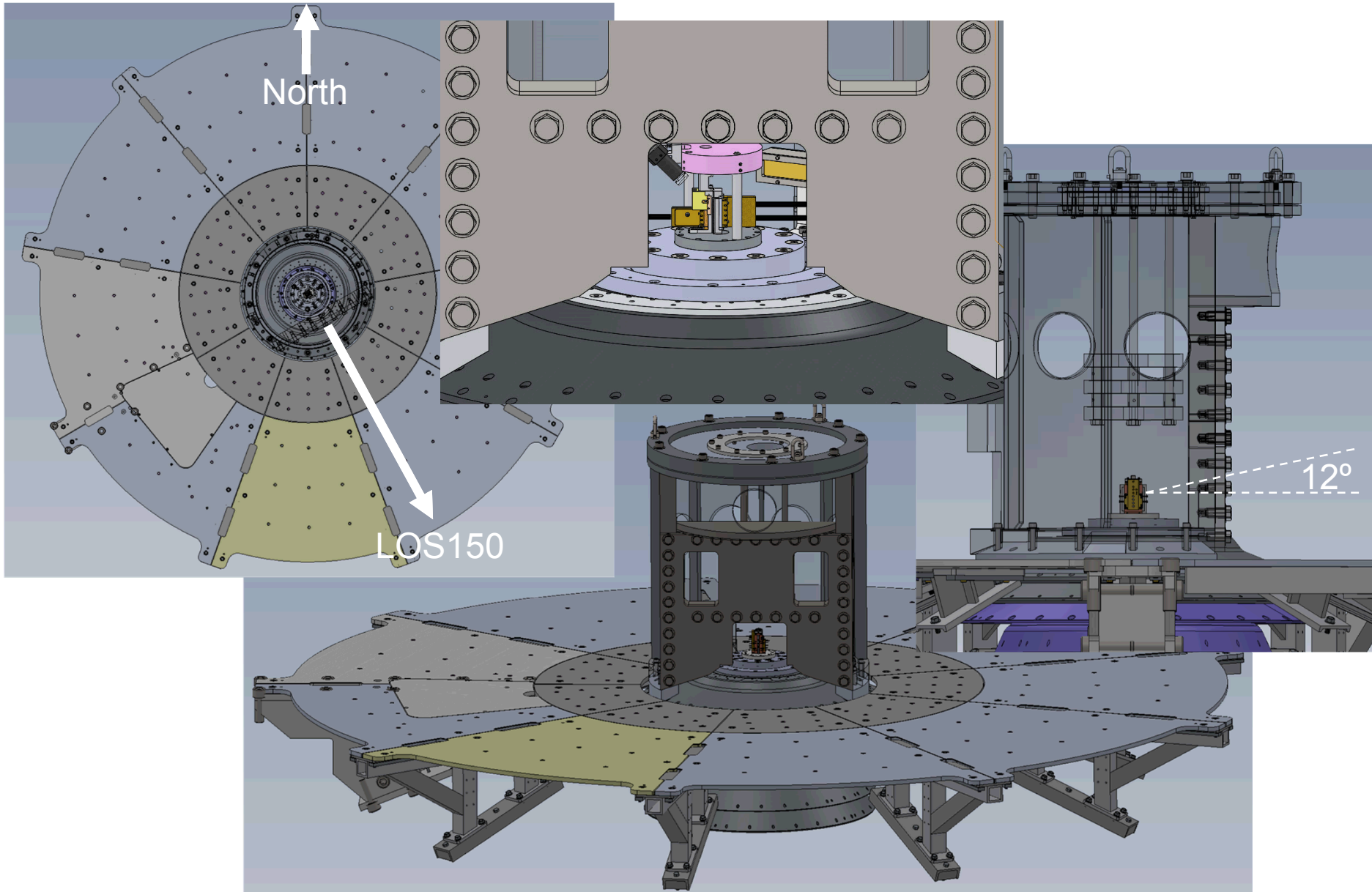
- Management POC: Chris Bourdon
- Responsible Scientist: Armon McPherson

Optical image relay

- Open optical beam propagation
 - Z-DMP load
 - Blast shield
 - Center section



Compatibility with Z-XRTS blast shield



Ongoing Work and Developments

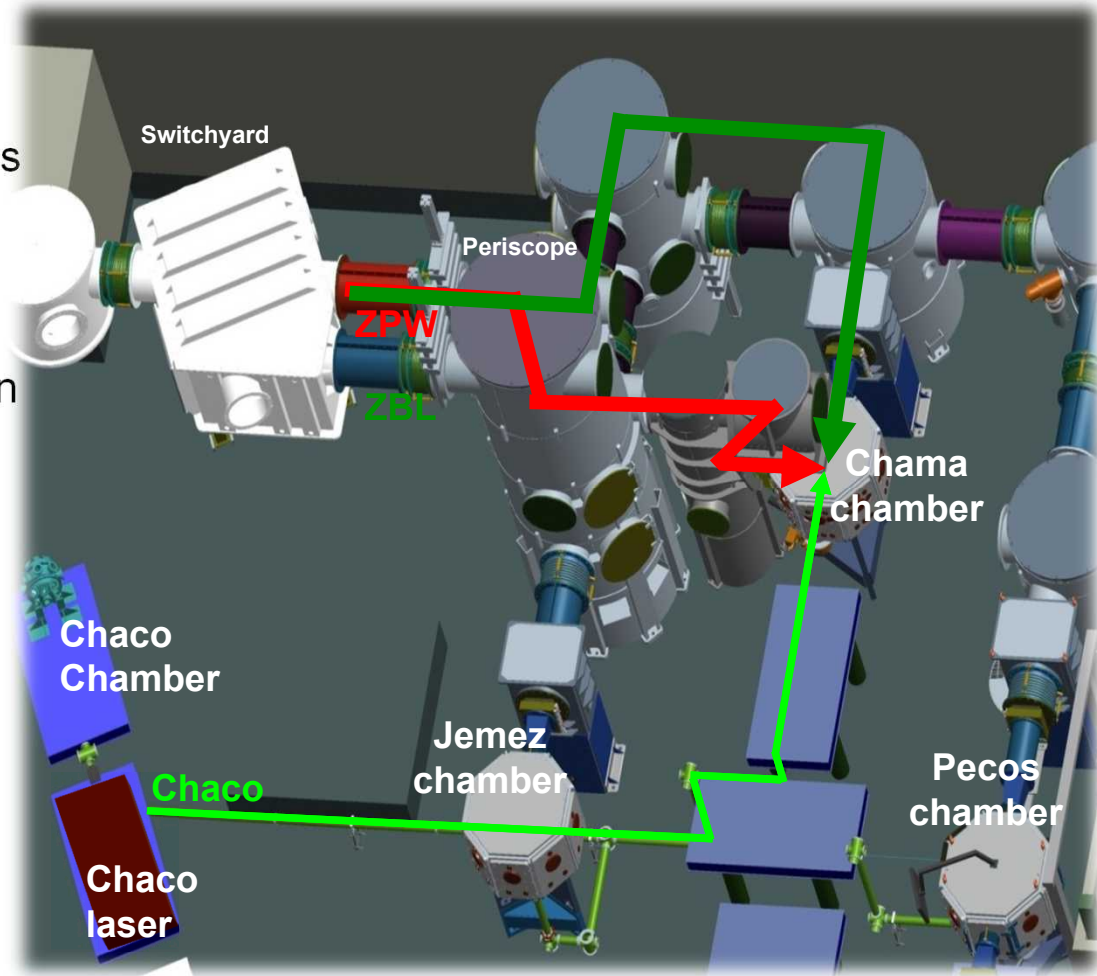
Laser-driven DXRD experiments

- New Chama target chamber for offline DXRD experiments
 - Anticipated activation: CY2017-Q1

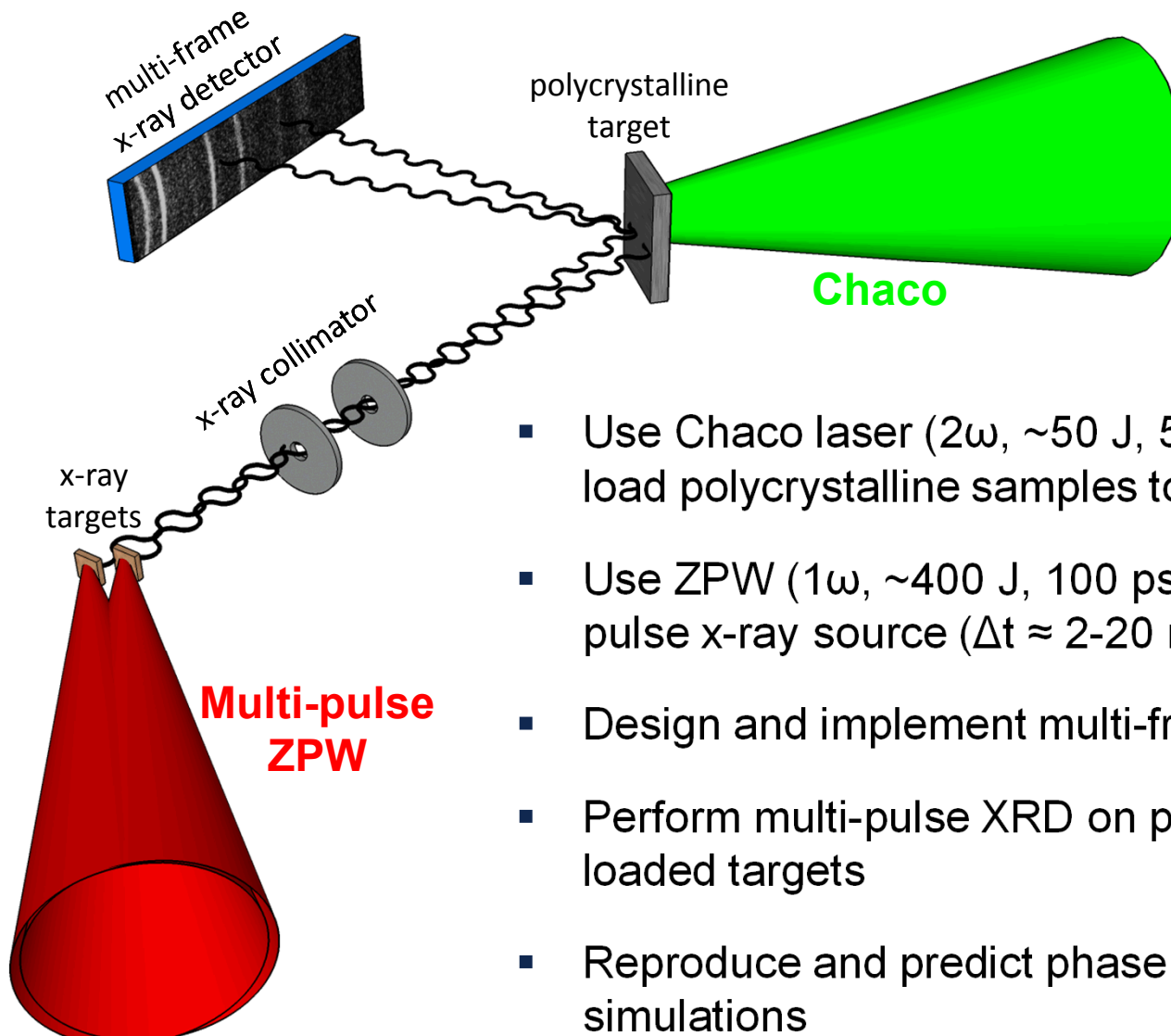
- Baseline plan
 - **ZPW** to create x-ray source
 - Up to $\sim 400\text{J}/1054\text{nm}/50\text{-}200\text{ps}$
 - Energy is limited due to gold gratings and B-integral issues in final focal lens

 - **Chaco** laser to drive diffraction targets
 - Up to $\sim 50\text{J}/532\text{nm}/5\text{-}10\text{ns}$

- Future plan
 - **ZBL** laser to drive diffraction targets
 - Up to $\sim 4\text{ kJ}/527\text{nm}/1\text{-}4\text{ns}$



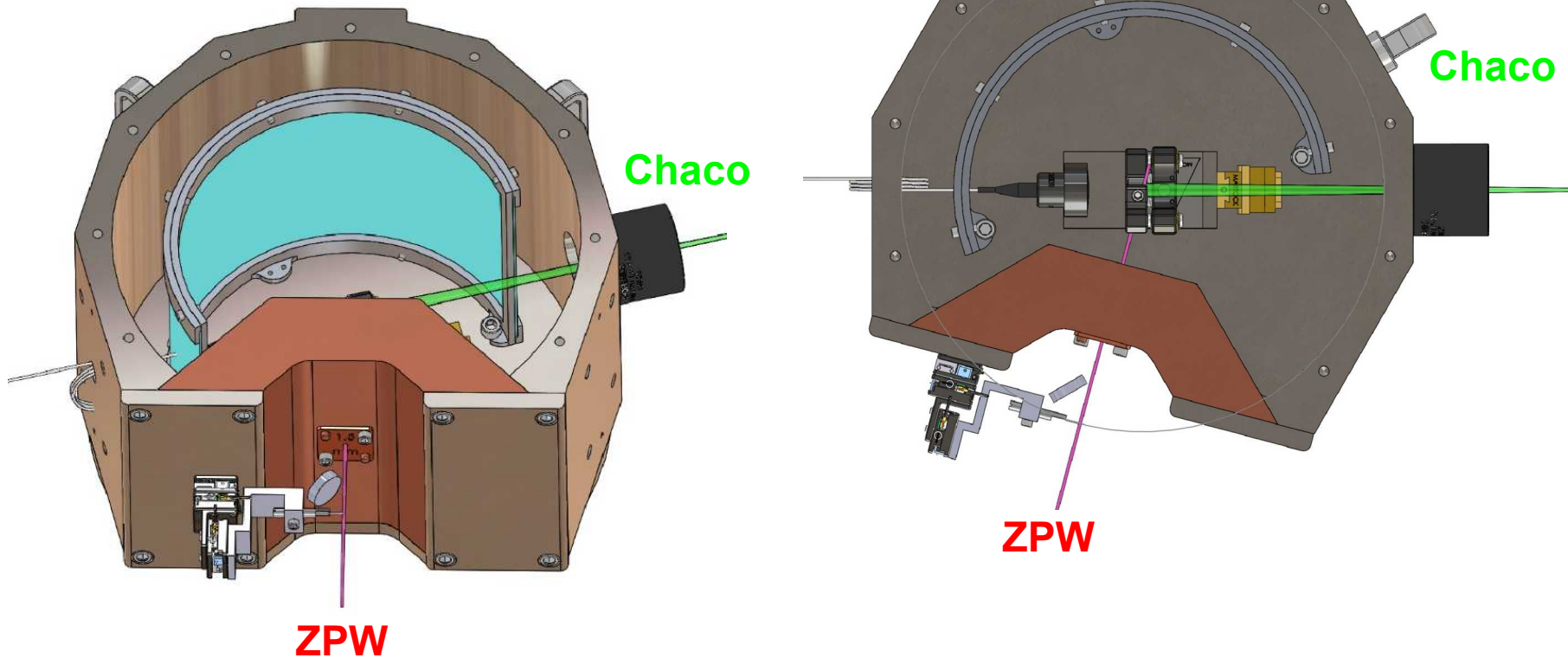
Conceptual design of laser-driven DXRD



- Use Chaco laser (2ω , ~ 50 J, 5-10 ns) to shock/ramp load polycrystalline samples to 10-20 GPa
- Use ZPW (1ω , ~ 400 J, 100 ps) laser to create multi-pulse x-ray source ($\Delta t \approx 2$ -20 ns)
- Design and implement multi-frame, 2D x-ray detector
- Perform multi-pulse XRD on polycrystalline, pressure-loaded targets
- Reproduce and predict phase transition dynamics with simulations

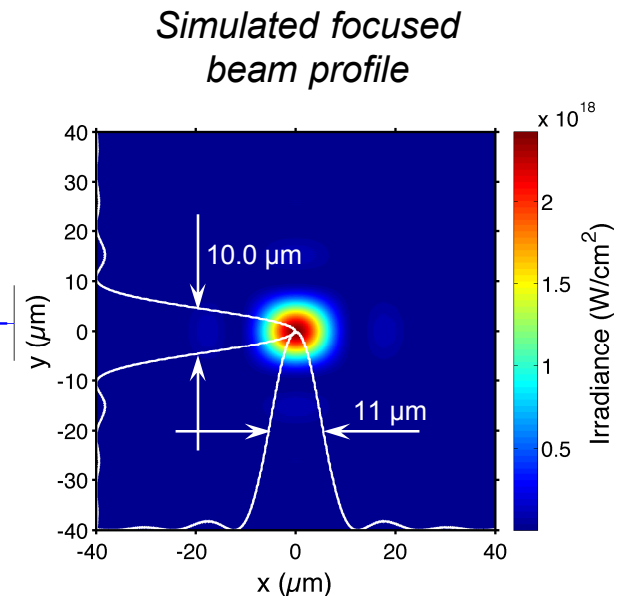
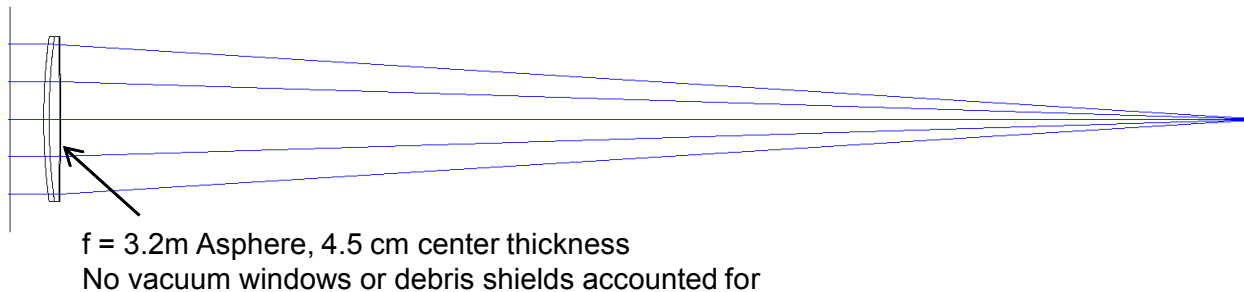
Phase And Crystallographic Measurement ANalyzer (PACMAN)

- 8 cm inner radius, 10 cm tall
- Thick shielding from ZPW source:
 - 3/8" stainless steel + 1" CuW (30/70)
- 3D-printed image plate holders for different radii
- Variable x-ray collimator sizes
- Motorized xyz for x-ray source



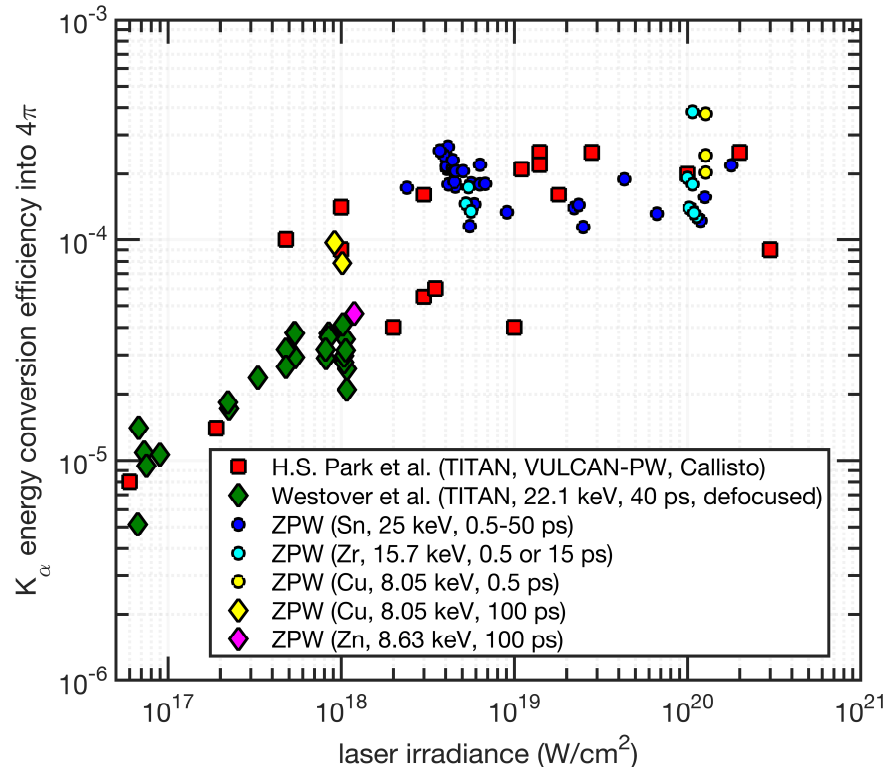
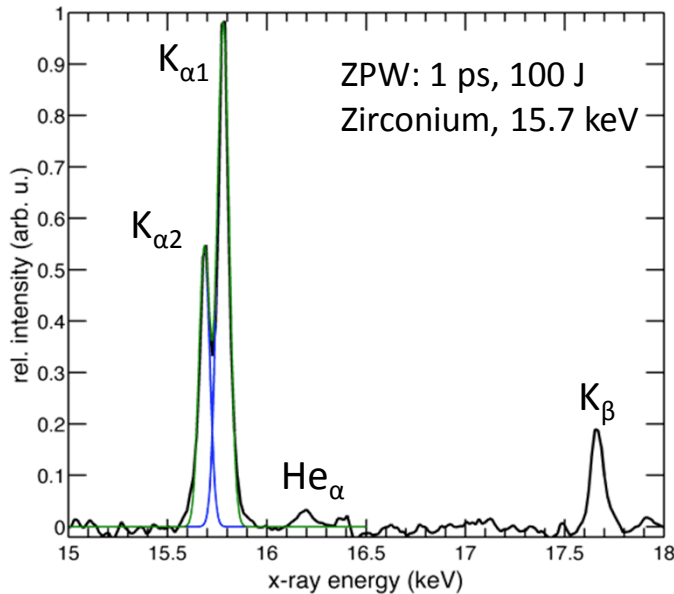
Lens focusing of ZPW to generate K α x-ray source

- ZPW provides **additional** beams for Z activities in conjunction with ZBL's 2ω beam:
 - Co-propagating 2ω full aperture beam (\sim ns, under construction)
 - Co-propagating 1ω full aperture beam (\sim 100ps, under construction)
- Note that a dual beam ZPW does *not* preclude dual frame ZBL operation
- Zemax modeling with the existing ZBL lens to focus a 10 TW (1 kJ/ 100 ps) ZPW beam indicates:
 - $\approx 1.2 \times 10^{10}$ W/cm² at the lens (matches B-Integral model)
 - $\approx 8 \times 10^{18}$ W/cm² at the best focus
 - focal spot: 11 μ m \times 10 μ m (FWHM)



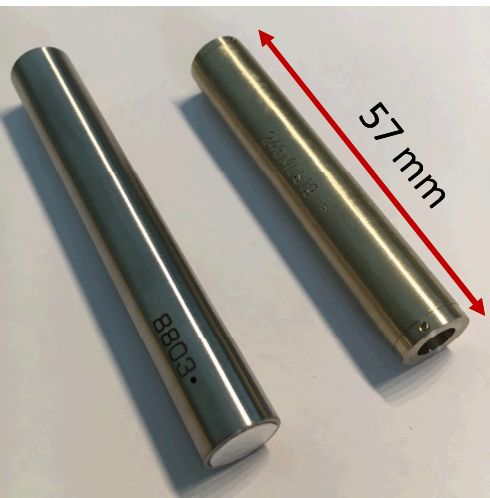
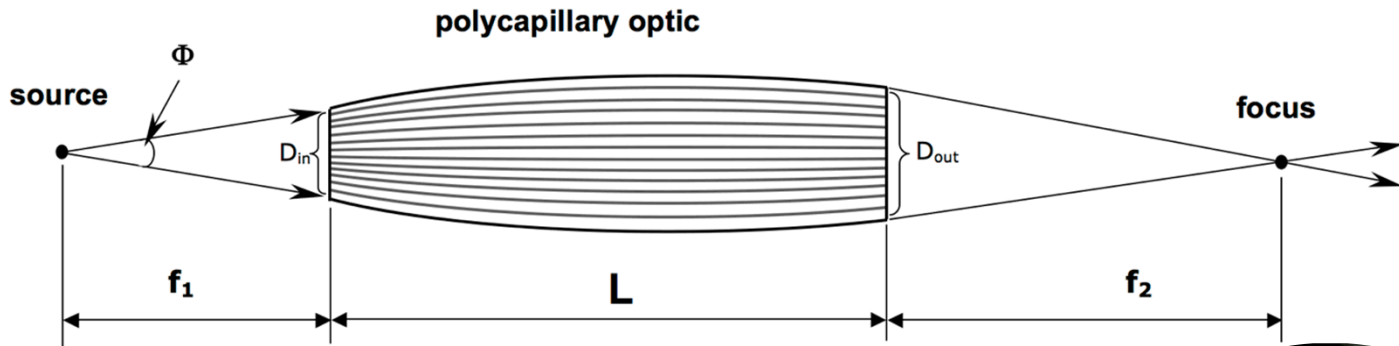
Verification of short pulse laser to x-ray energy conversion efficiency of ZPW

- ZPW operates between 0.5 and 100 ps pulse duration, best focus (5.6 μm FWHM)
- X-ray yield measured with single photon counting CCD (Princeton Instruments PI-LCX:1300)

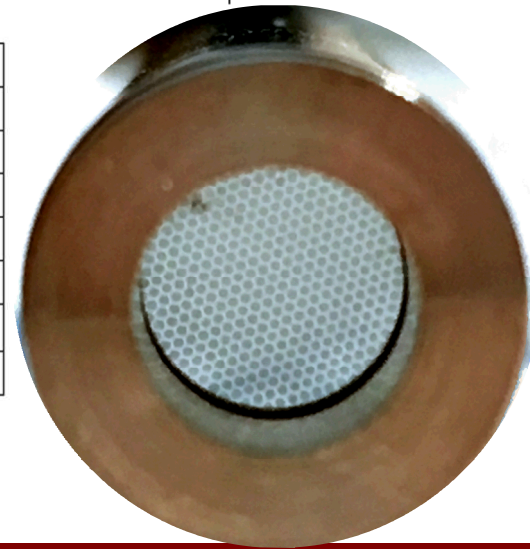


X-ray polycapillaries for flux enhancement and background suppression

- Convert a highly divergent beam into a quasi-parallel beam with low divergence
 - X-ray energy range: ~1–30 keV
 - Solid collection angle: up 20°
 - Intensity gain: ~30–100X



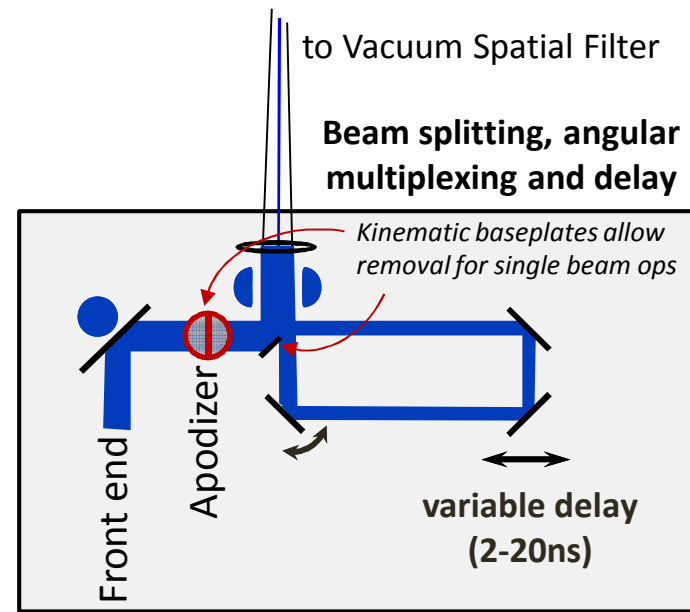
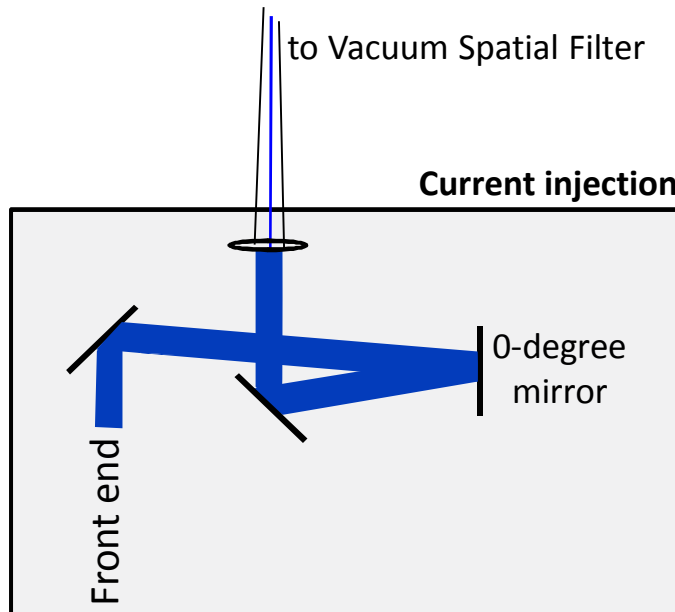
f_1 , mm	31.3
f_2 , mm	105
L , mm	48.7
D_{in} , mm	4.75
D_{out} , mm	6.8
D_{max} , mm	7.25
Φ , rad	0.151
$R = f_1 + f_2 + L$, mm	185



Vendors: XOS, IfG

Multi-frame ZPW modification

- Concept and implementation
 - Spatially split beam before injection into main amp section
 - Full delay adjustment ($\approx 2-20$ ns)
 - *Separated* far-field spots (2 targets)
 - Similar to Z-Beamlet multi-frame backlighter (MFB) concept but without certain energy losses (except for apodization strip at 10% level)
 - Compatible with grating compressor
 - Allows 2 beams with each at 500J/0.1ns or 1kJ/0.2ns (B-integral limited)



Evaluation of scintillators/phosphors

Detector	Chemical Formula	1/e Decay Time	Light Wavelength (nm)	Light Yield (photon/keV)	Dynamic Experiments
Image Plate BAS-MS	BaFBr _{0.85} I _{0.15} :Eu ²⁺	-	400	5 mPSL	✓
MCP	SiO ₂ :Pb	< 1 ns	-	-	✓
Mirrored P-43	Gd ₂ O ₂ S:Tb	1 ms	550	95	✓
Mirrored P-47	Y ₂ SiO ₃ :Ce	50 ns	450	38	
Microcolumnar CsI	CsI:Tl	1000 ns	550	54	
LSO	Lu ₂ SiO ₅ :Ce ³⁺	47 ns	400	30	✓
PreLude420	Lu _{1.8} Y ₂ SiO ₅ :Ce	41 ns	420	32	
BriLanCe380	LaBr ₃ :Ce	16 ns	380	63	
ZnO:Ga	ZnO:Ga	0.8 ns	385	9	
New LBL	(?)	< 0.2 ns	540	~0.2	

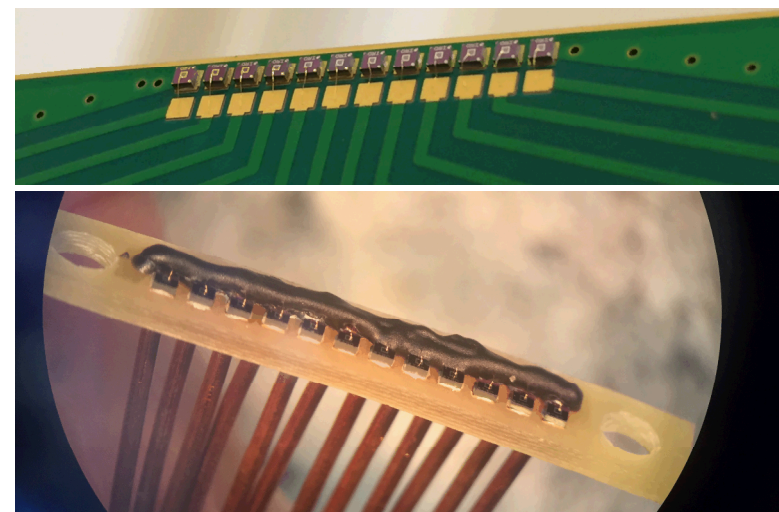
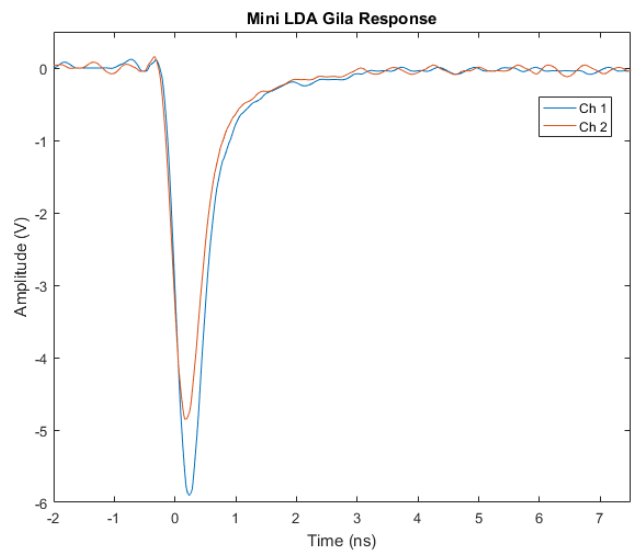
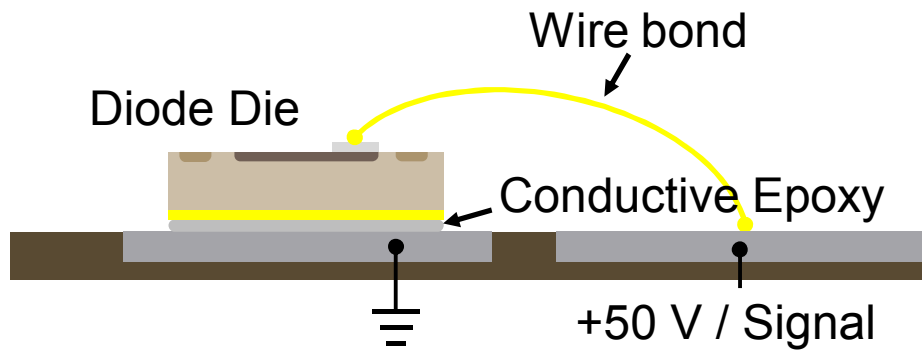
Fielding of CCD camera on Z

- Princeton Instruments PI-MAX4: Intensified gated CCD camera
 - Number of pixels: 2048 x 2048 imaging array
 - Pixel size: 13.5 μm x 13.5 μm
 - Format size: 27.6 mm x 27.6 mm (39 mm diagonal)
 - Intensifier resolution limit: 40 to 64 lp/mm
 - Minimum gate width: \sim 4 ns
 - Timing resolution / jitter: 10 ps / 35 ps
- Operational testing on Z-DMP ridealongs
 - Robustness to Z shots
 - Electromagnetic pulse
 - Physical vibrations
 - Signal-to-noise
 - X-ray background
 - Visible light background



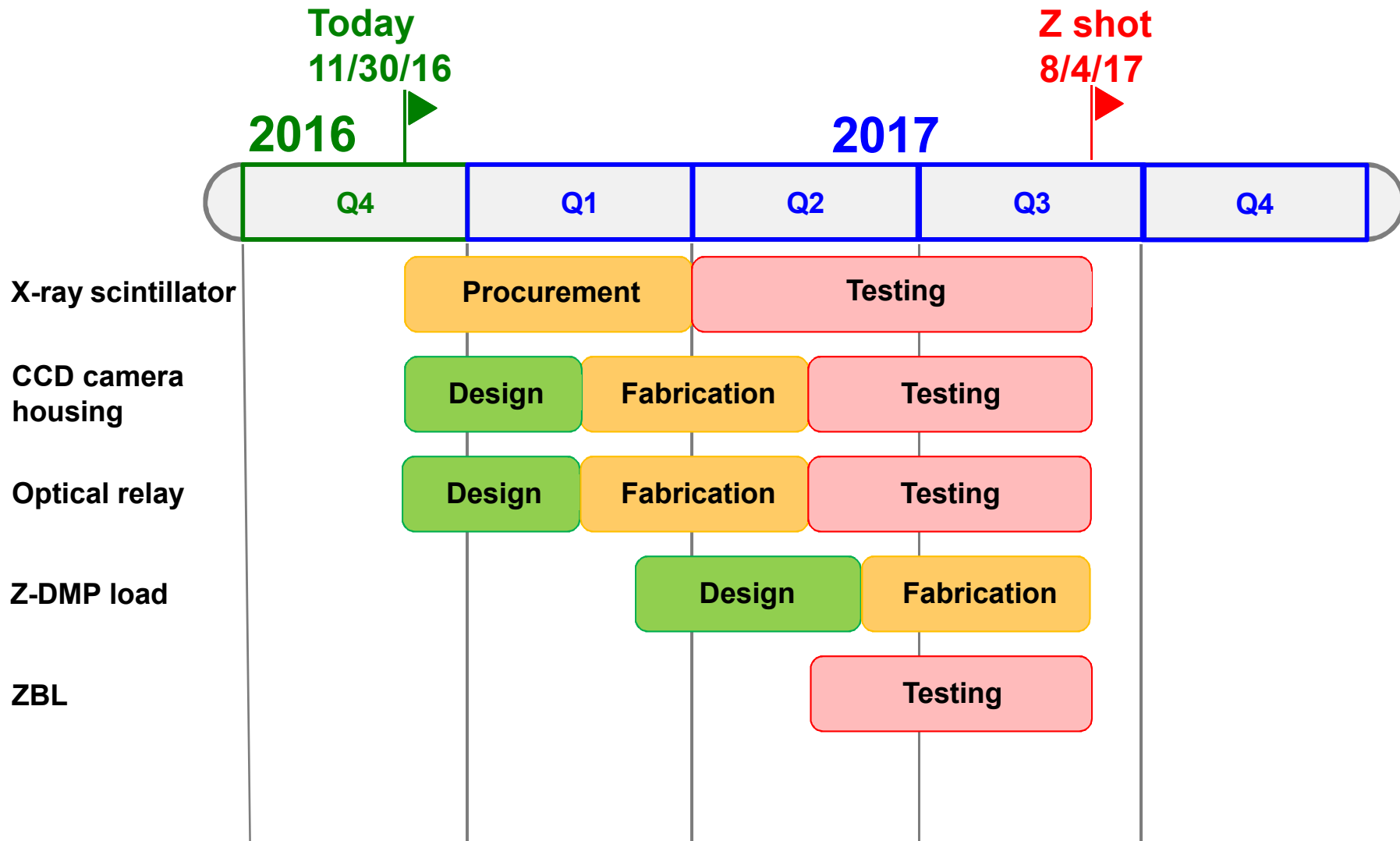
Time-resolved DXRD using direct x-ray detection linear diode array (LDA)

- Hybrid XRD detector
 - Scintillator/CCD camera: 2D XRD pattern, time-gated
 - LDA: 1D XRD line, sub-ns time-resolution



- Visible light testing
 - Gila laser 532 nm
 - ~200 ps in duration
- 12 discrete diodes, up to 1 mm die size, linear spacing 1.6 mm pitch
- Integrated biasing circuit
- Designed for >3 GHz bandwidth

Timeline for 1st Z-XRD experiment



Extra Slides

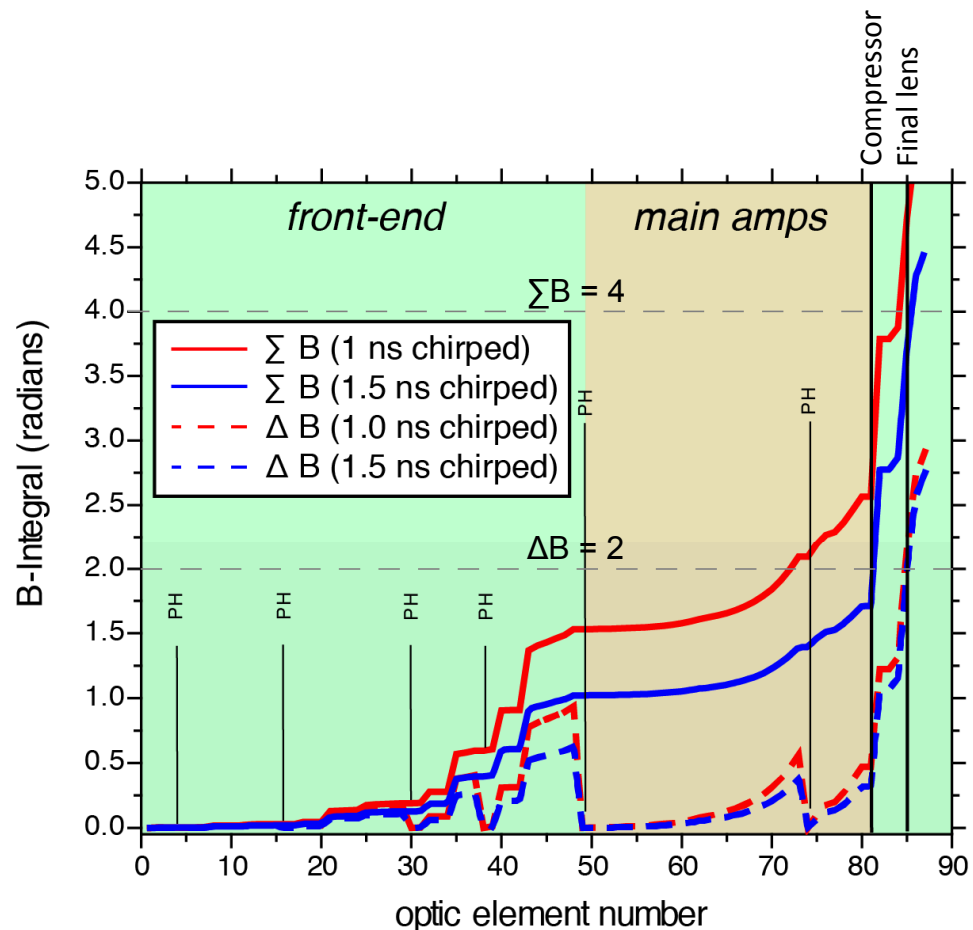
B-Integral considerations

- Refractive index depends on intensity: $n(I) = n_0 + n_2 I$
- Intense laser propagation then has a nonlinear component to phase ($\Phi = 2\pi/\lambda n(I) z$), which accumulates (called B-integral):

$$B = \frac{2\pi}{\lambda} \int_0^L n_2(z)I(z) dz$$

- Limits:
 - Total accumulated nonlinear phase must be $\sum B < 4$ to avoid whole-beam self-focusing effects (i.e., focal spot shifting)
 - “small” spatial defects can be stripped at pinholes of spatial filters. B-integral between pinholes resets to 0 at each pinhole. Keep $\Delta B < 2$

⇒ Amplify pulse with 1-1.5 ns chirp, then compress to ≈ 100 ps prior to focusing



Other ZPW multi-frame ideas

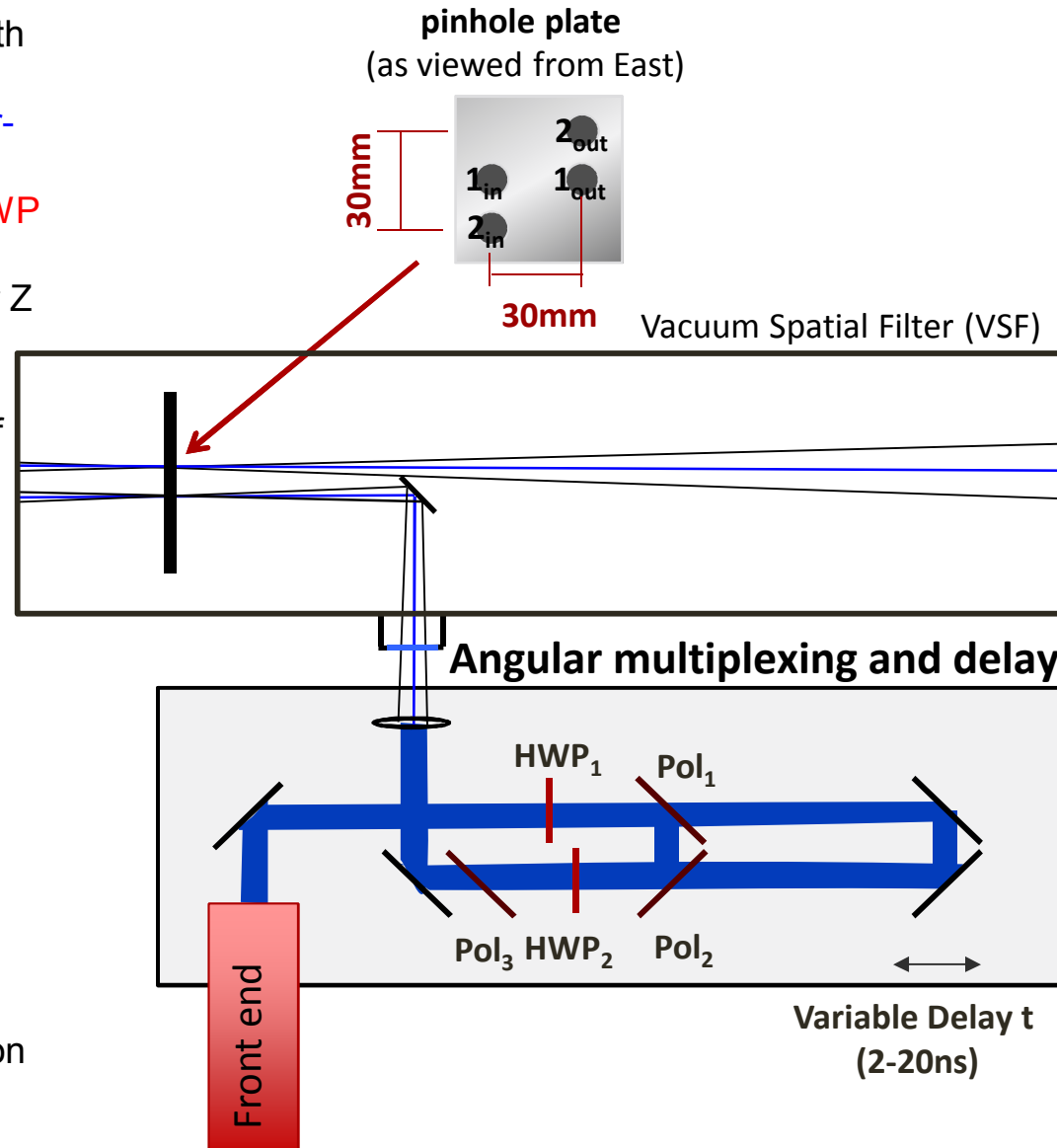
Option 1: Replace single-pulse VSF injection with dual-pulse

- full delay adjustment with separated far-field spots
- **Loses 1/2 of the beam energy due to HWP**
- ~500J/pulse after compression
- proof of concept, but maybe too low for Z

Option 2: Same approach, much earlier in front end using a fast rise-time Pockels cell in place of HWP

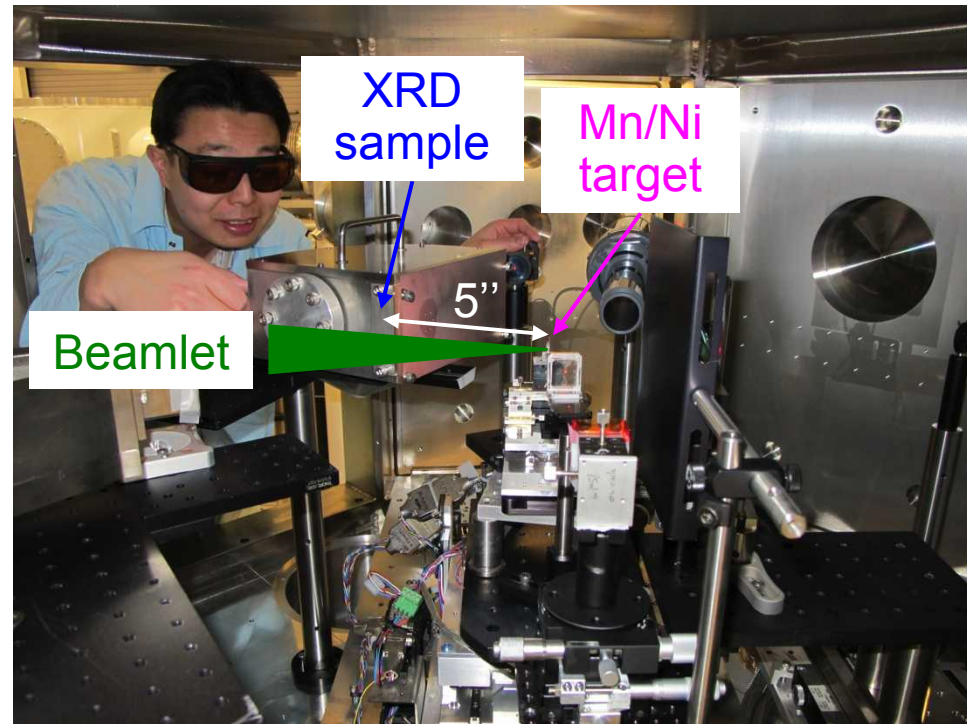
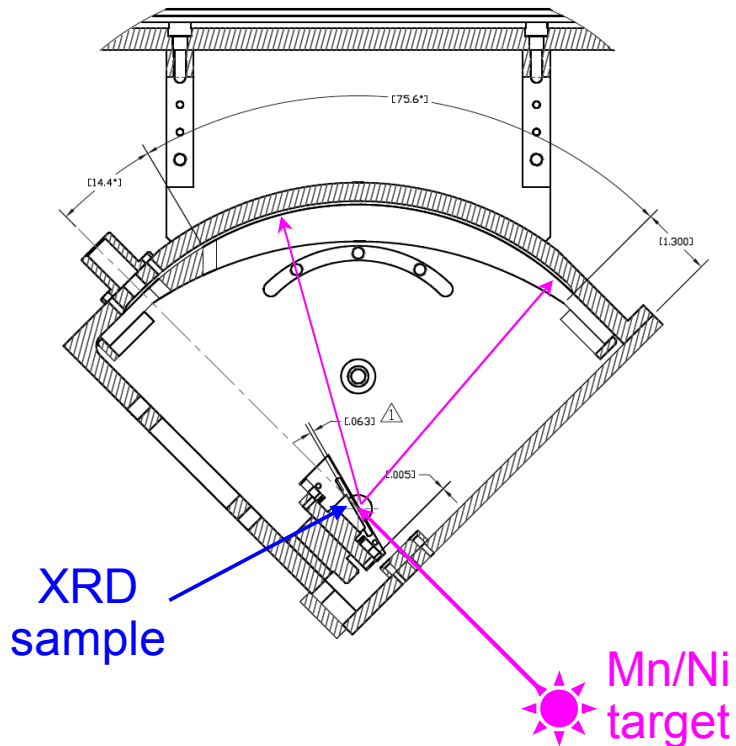
- gets rid of the loss of 1/2 of the beam
- **the pulses must be co-bored to get through the rod amplifiers/VSF's in the front-end**
- increases the energy per pulse, but restricts the pulses to be co-bored
- **pulse delays limited to 4-5 ns due to main amp pinhole closure**
- Could increase to 20ns with NIF-style high-Z conical PH's
- **Implementation may be cheaper**

Careful evaluation of pro's/con's and final decision will be done in first year of LDRD

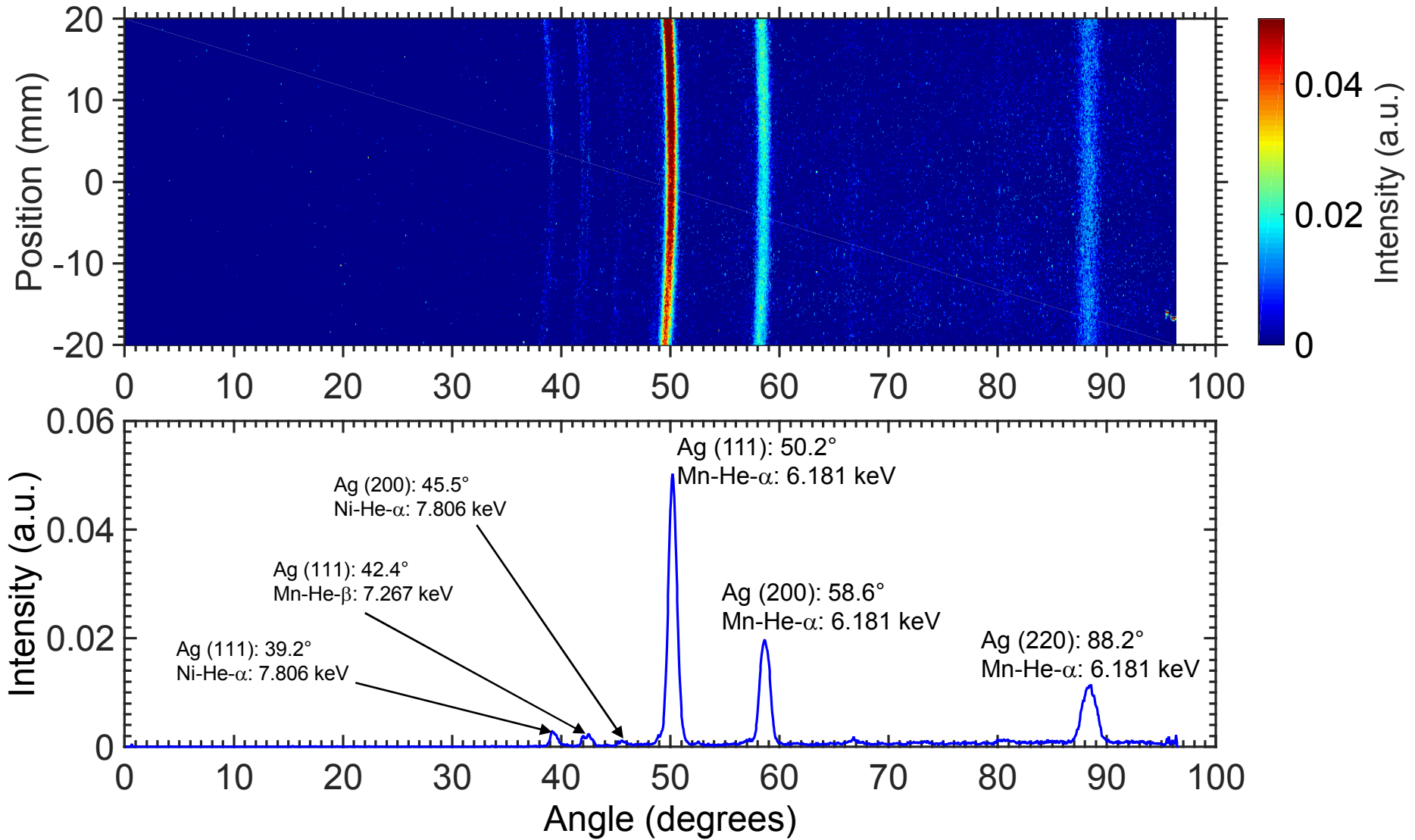


XRD using Z-Beamlet in Jemez chamber

- Z-Beamlet: 1-2 kJ, 1-2 ns
 - Mn(88%)/Ni(12%) foils
 - Mn-He- α : 6.181 keV, Mn-He- β : 7.267 keV; Ni-He- α : 7.806 keV
- NSTec XRD quadrant box
 - Polycrystalline metal samples (Ag, Al, Fe, Cu, Ce)



B15120903: XRD of ambient Ag (fcc) sample



Photometric calculations for Ag

Current ZBL source:

- Mn He_α (E = 6.181 keV)
- **Source brightness: $5e-3 \times 1500 \text{ J} \rightarrow \approx 10^{16}$ photons**

Pinhole ($\phi = 1.2 \text{ mm}$) distance: 5" (12.7 cm)

Pinhole solid angle $\Omega = 6 \times 10^{-6} \text{ sr}$

Photons incident on sample: 6×10^{10}

Coherent scattering cross section: $\sigma = 700 \text{ barns/atom}$ [1]

He_α attenuation length [2]: $\mu = 1.0 \text{ }\mu\text{m}$

Ag atomic number density: $n = \rho \times N_{av}/M = 5.9 \times 10^{22} \text{ cm}^{-3}$

Total scattering fraction $F = \mu/2 \times n \times \sigma \approx 0.002$

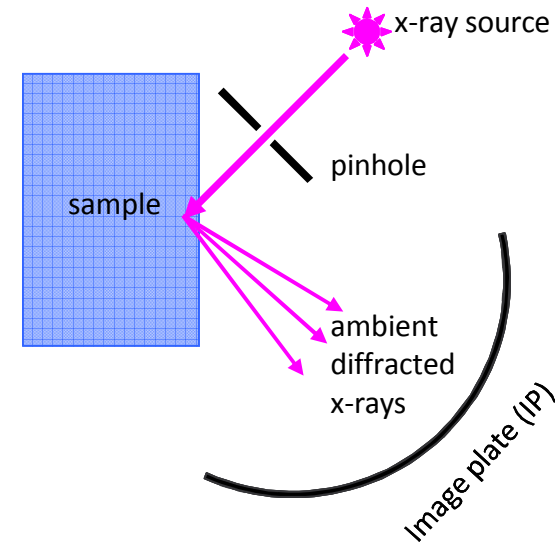
Solid angle of 1 pixel at detector (5" distance, $50 \times 50 \text{ }\mu\text{m}^2$): $\approx 10^{-8} \text{ sr}$

Total collected photons per pixel: $6 \times 10^{10} \times 0.002 \times 10^{-8} \approx 1.2$

TR-IP sensitivity at 6 keV: $\approx 3.3 \text{ mPSL}/\gamma$

→ **Expected signal: $\approx 0.004 \text{ PSL}$**

→ **Measured signal: $\approx 0.01 \text{ PSL}$**



Photometric calculations for Ag using ZPW

Current ZPW source:

- Zr He_α (E = 15.7 keV)
- **Source brightness: $1e-4 \times 500 \text{ J} \rightarrow \approx 5 \times 10^{13}$ photons**

Pinhole ($\phi = 1.2 \text{ mm}$) distance: 2" (5 cm)

Pinhole solid angle $\Omega = 3.6 \times 10^{-5} \text{ sr}$

Photons incident on sample: 1.8×10^9

Coherent scattering cross section: $\sigma = 300 \text{ barns/atom}$ [1]

K_α attenuation length [2]: $\mu = 7.5 \mu\text{m}$

Ag atomic number density: $n = \rho \times N_{av}/M = 5.9 \times 10^{22} \text{ cm}^{-3}$

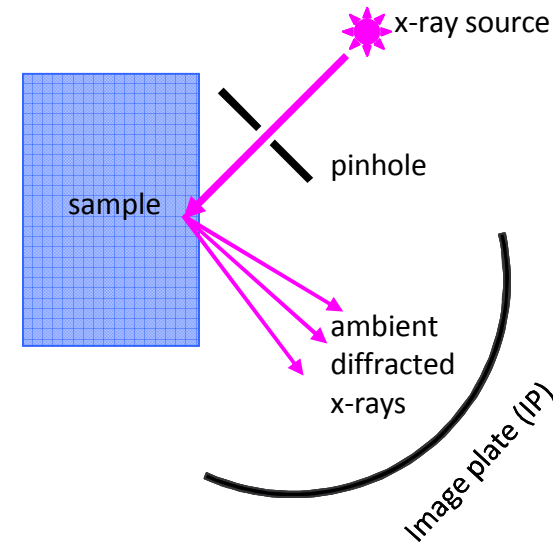
Total scattering fraction $F = \mu/2 \times n \times \sigma \approx 0.0066$

Solid angle of 1 pixel at detector (2" distance, $50 \times 50 \mu\text{m}^2$): $\approx 8 \times 10^{-8} \text{ sr}$

Total collected photons per pixel: $1.8 \times 10^9 \times 0.0066 \times 8 \times 10^{-8} \approx 1$

MS-IP sensitivity at 15 keV: $\approx 10 \text{ mPSL}/\gamma$

→ **Expected signal: $\approx 0.01 \text{ PSL}$**



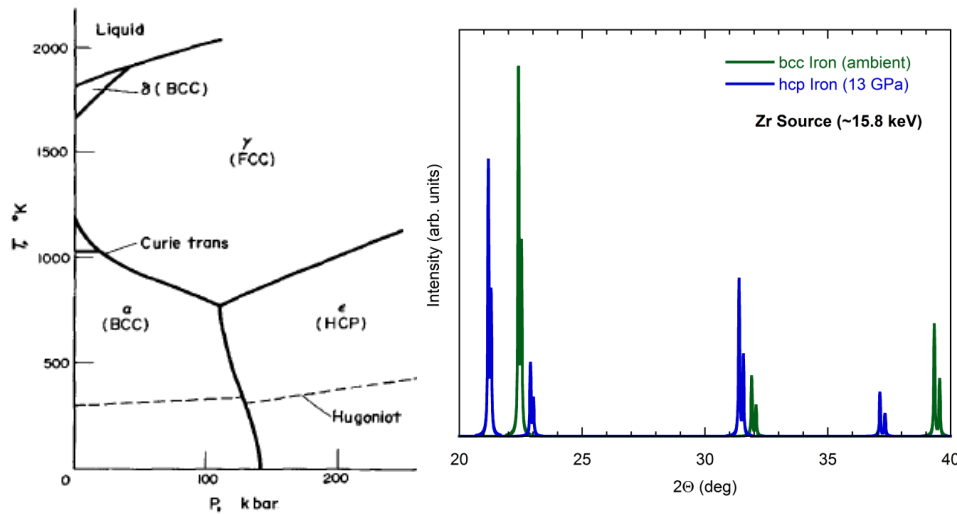
Examples of possible Z-XRD experiments

- Ramp experiments: solid-solid phase transitions
 - Iron
 - Zirconium
 - Lithium
- Shock-ramp: liquid to re-solidification
 - Tin
 - Cerium
- Use XRD as new melting diagnostic on Hugoniot for metals

Z-XRD ramp experiments

Iron

- Exhibits $\alpha(\text{bcc}) \rightarrow \epsilon(\text{hcp})$ phase transition on Hugoniot and principle isentrope at $\sim 13 \text{ GPa}$



D. H. Kalantar, *et al.*, Phys. Rev. Lett. **95**, 075502 (2005)
 J. Hawreliak *et al.*, PRB **83**, 144114 (2011)

Zirconium

- Exhibit $\alpha(\text{hcp}) \rightarrow \omega(\text{hex})$ phase transition on Hugoniot and principle isentrope at $\sim 2-11 \text{ GPa}$
- The $\omega(\text{hex}) \rightarrow \beta(\text{bcc})$ phase transition occurs at different locations on Hugoniot ($\sim 25 \text{ GPa}$) and isentrope ($\sim 30 \text{ GPa}$)

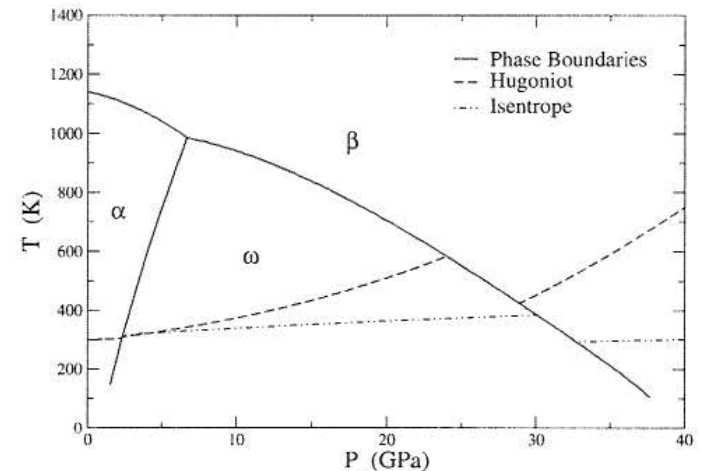


FIG. 1. Calculated phase diagram and Hugoniot for the three solid phases of zirconium using the EOS developed by Greeff (Ref. 8).

P. A. Rigg *et al.*, J. Appl. Phys. **106**, 123532 (2009)
 D. Morgan *et al.*, Powder Diffraction **25**, 138 (2010)

Z-XRD shock-ramp experiments

Tin

- Shock melt (~50 GPa) to liquid, ramp compress (~100 GPa) to refreeze into bct-Sn or bcc-Sn

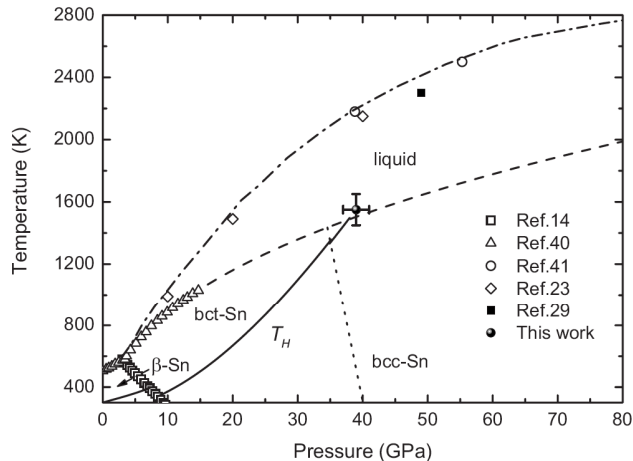
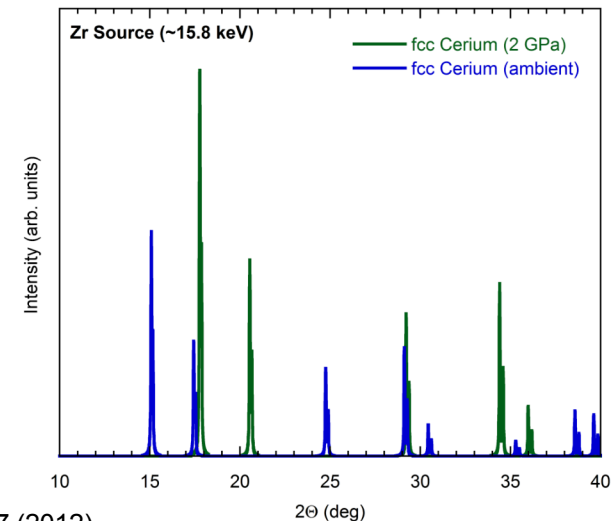
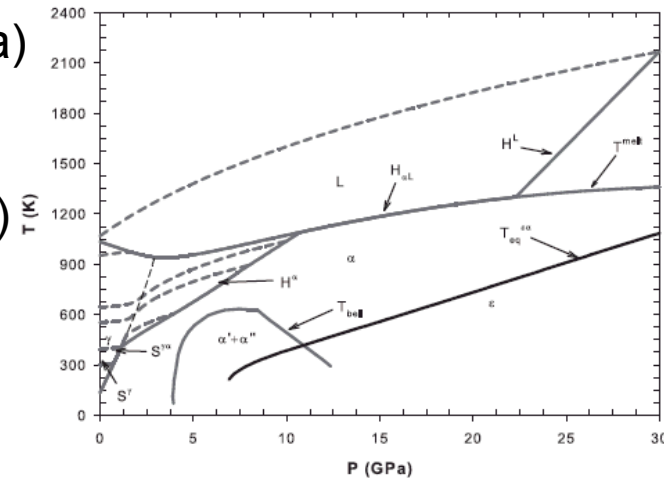


FIG. 6. A tentative phase diagram of tin. The solid line is the calculated Hugoniot temperatures using Eqs. (6a)–(6c). The dashed line is the extrapolation of DAC experimental results according to Simon melting equation. The Dash-dot line is the melt curve given in Ref. 41. The dot line is the tentative phase boundary between bct and bcc phase.

J. Hu *et al.*, JAP **104**, 083520 (2008)
D. Morgan *et al.*, RSI **79**, 113904 (2008)

Cerium

- Shock melt (~20 GPa) to liquid, ramp compress (~50 GPa) to refreeze into α (fcc)
- Exhibits an isostructural (fcc) phase transition $\odot \rightarrow \langle$ on the principal isentrope at ~2 GPa with ~15% volume collapse
- Low pressure phase change useful for testing XRD schemes at ZBL and DICE

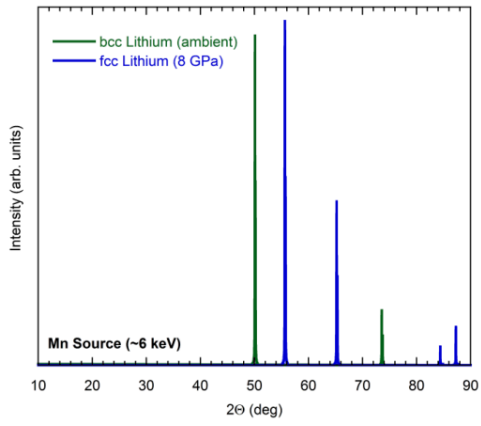
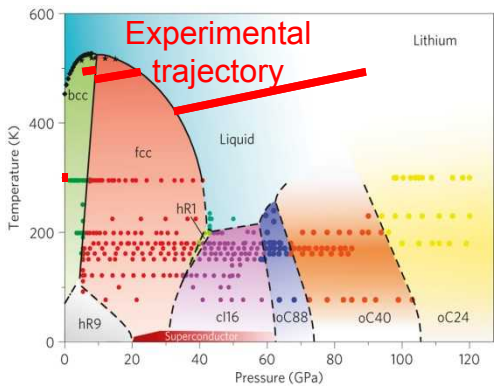


F. Decremps *et al.*, PRL **106**, 065701 (2011)
A. V. Nikolaev *et al.*, Physics Uspekhi **55**, 657 (2012)

Possible first Z-XRD experiments could use Beamlet generated 6-8 keV x-rays

Lithium

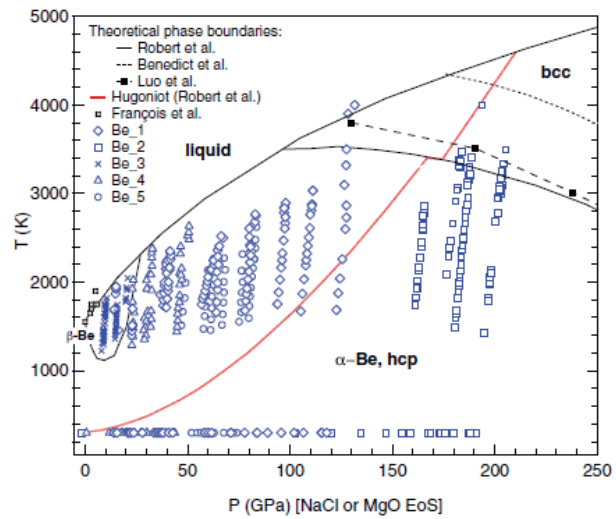
- Lithium has very low mass attenuation coefficient (probe ~1 mm thickness)
- Timed correctly, a two-phase pattern (bcc/fcc) may be observed
- Free surface ramp compression with XRD diagnostic timed to probe bcc-fcc phase transition



C. L. Guillaume *et al.*, Nature Physics 7, 211 (2011)

Beryllium

- Beryllium also has low mass attenuation coefficient, but no phase transitions with ramp; XRD should see compression of the hcp lattice
- Alternatively, attempt to shock into bcc, probe before free surface breakout



Hugoniot may not intersect bcc?

A. Lazicki *et al.*, PRB 86, 174118 (2012)

Photometric calculations for Zr using ZBL

Current ZBL source:

- Mn He_α (E = 6.181 keV)
- **Source brightness: $5e-3 \times 1500 \text{ J} \rightarrow \approx 10^{16}$ photons**

Pinhole ($\phi = 1.2 \text{ mm}$) distance: 5" (12.7 cm)

Pinhole solid angle $\Omega = 6 \times 10^{-6} \text{ sr}$

Photons incident on sample: 6×10^{10}

Coherent scattering cross section: $\sigma = 480 \text{ barns/atom}$ [1]

He_α attenuation length [2]: $\mu = 2.4 \mu\text{m}$

Zr atomic number density: $n = \rho \times N_{av}/M = 4.3 \times 10^{22} \text{ cm}^{-3}$

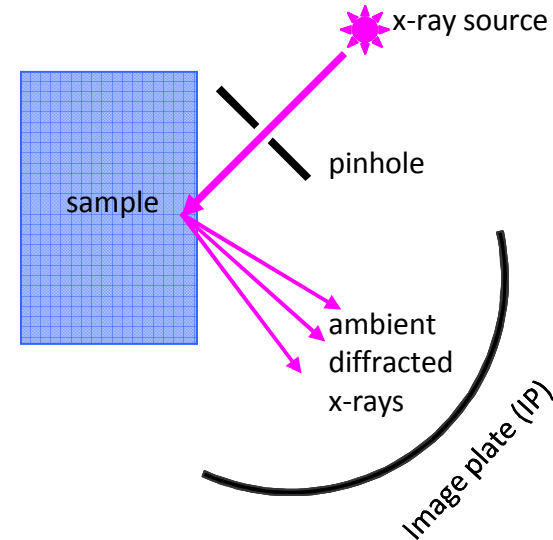
Total scattering fraction $F = \mu/2 \times n \times \sigma \approx 0.0025$

Solid angle of 1 pixel at detector (5" distance, $50 \times 50 \mu\text{m}^2$): $\approx 10^{-8} \text{ sr}$

Total collected photons per pixel: $6 \times 10^{10} \times 0.0025 \times 10^{-8} \approx 1.5$

TR-IP sensitivity at 6 keV: $\approx 3.3 \text{ mPSL}/\gamma$

→ **Expected signal: $\approx 0.005 \text{ PSL}$**



Photometric calculations for Ti using ZBL

Current ZBL source:

- Mn He_α (E = 6.181 keV)
- **Source brightness: $5e-3 \times 1500 \text{ J} \rightarrow \approx 10^{16}$ photons**

Pinhole ($\phi = 1.2 \text{ mm}$) distance: 5" (12.7 cm)

Pinhole solid angle $\Omega = 6 \times 10^{-6} \text{ sr}$

Photons incident on sample: 6×10^{10}

Coherent scattering cross section: $\sigma = 100 \text{ barns/atom}$ [1]

He_α attenuation length [2]: $\mu = 2.3 \mu\text{m}$

Ti atomic number density: $n = \rho \times N_{av}/M = 5.7 \times 10^{22} \text{ cm}^{-3}$

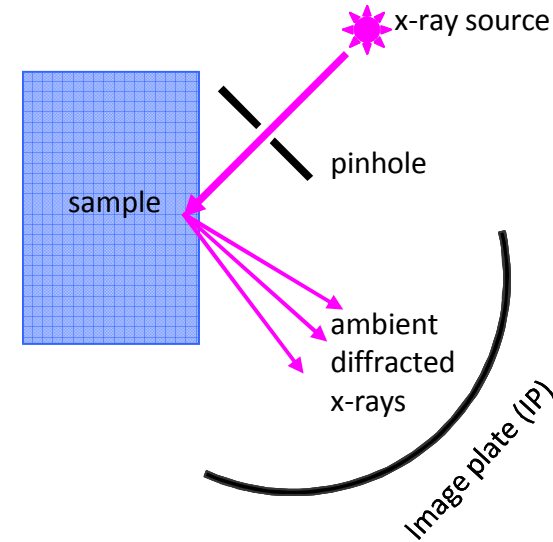
Total scattering fraction $F = \mu/2 \times n \times \sigma \approx 0.0007$

Solid angle of 1 pixel at detector (5" distance, $50 \times 50 \mu\text{m}^2$): $\approx 10^{-8} \text{ sr}$

Total collected photons per pixel: $6 \times 10^{10} \times 0.0007 \times 10^{-8} \approx 0.4$

TR-IP sensitivity at 6 keV: $\approx 3.3 \text{ mPSL}/\gamma$

→ **Expected signal: $\approx 0.001 \text{ PSL}$**



Photometric calculations for Be using ZBL

Current ZBL source:

- Mn He_α (E = 6.181 keV)
- **Source brightness: $5e-3 \times 1500 \text{ J} \rightarrow \approx 10^{16}$ photons**

Pinhole ($\phi = 1.2 \text{ mm}$) distance: 5" (12.7 cm)

Pinhole solid angle $\Omega = 6 \times 10^{-6} \text{ sr}$

Photons incident on sample: 6×10^{10}

Coherent scattering cross section: $\sigma = 2.5 \text{ barns/atom}$ [1]

He_α attenuation length [2]: $\mu = 630 \text{ }\mu\text{m}$

Be atomic number density: $n = \rho \times N_{av}/M = 1.2 \times 10^{23} \text{ cm}^{-3}$

Total scattering fraction $F = \mu/2 \times n \times \sigma \approx 0.01$

Solid angle of 1 pixel at detector (5" distance, $50 \times 50 \text{ }\mu\text{m}^2$): $\approx 10^{-8} \text{ sr}$

Total collected photons per pixel: $6 \times 10^{10} \times 0.01 \times 10^{-8} \approx 3$

TR-IP sensitivity at 6 keV: $\approx 3.3 \text{ mPSL}/\gamma$

→ **Expected signal: $\approx 0.01 \text{ PSL}$**

